Karotáž
(well-logs)

Geologie sedimentárních pánví

(Geology of sedimentary basins)

LS (Summer term)

Karel Martínek

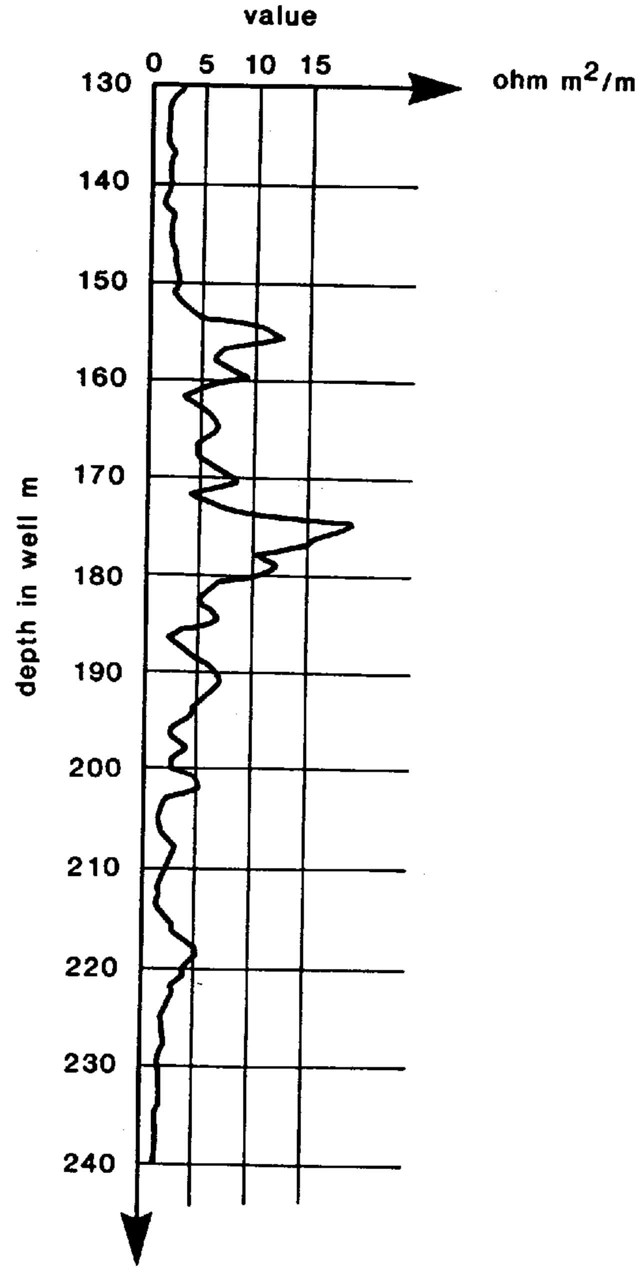

Figure 1.1 A well log. Representation of the first 'log' made at Pechelbronn, Alsace, France, in 1927 by H. Doll. (From Allaud and Martin, 1976).

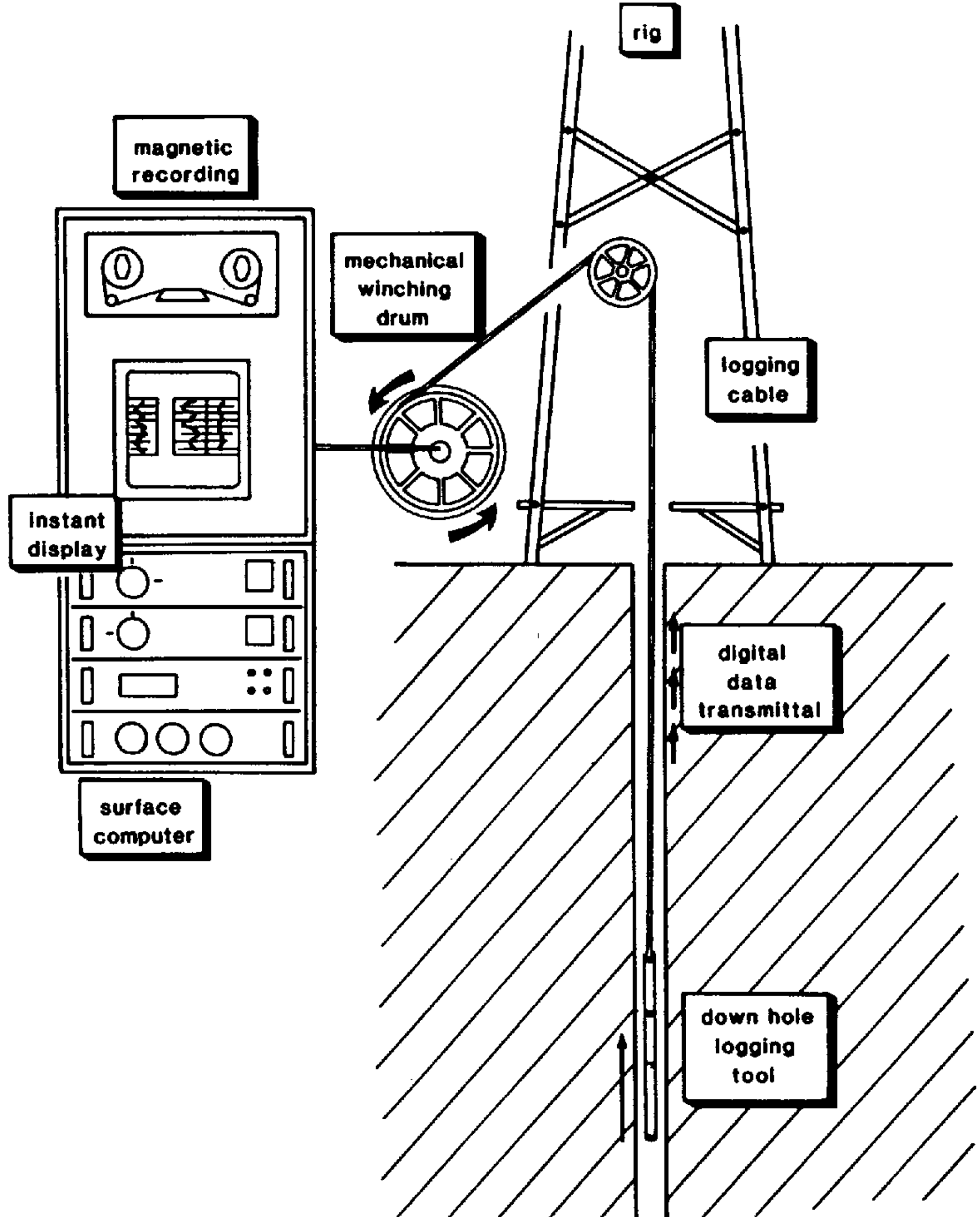

rig
magnetic recording
mechanical winching drum
logging cable
instant display
digital data transmittal
surface computer
down hole logging tool

Table 1.1 Classification of the common wireline geophysical well measurements (in 'open hole').

	Log Type	**Formation parameter measured**
Mechanical measurements	Caliper	Hole diameter
Spontaneous measurements	Temperature	Borehole temperature
	SP (self-potential)	Spontaneous electrical currents
	Gamma ray	Natural radioactivity
Induced measurements	Resistivity	Resistance to electrical current
	Induction	Conductivity of electrical current
	Sonic	Velocity of sound propagation
	Density	Reaction to gamma ray bombardment
	Photoelectric	Reaction to gamma ray bombardment
	Neutron	Reaction to neutron bombardment

Table 1.2 Principal uses of open-hole wireline logs.

Chapter	Uses	General geology						Reservoir geology		Geochemistry		Petrophysics						Seismic	
		Lithology – general	Volcanics (Unusual Lithology)	Evaporites (Unusual Lithology)	Mineral identification	Correlation: stratigraphy	Facies depositional env.	Fracture identification	Over-pressure identification	Source rock identification	Maturity	Porosity	Permeability	Shale volume	Fm. water salinity	Hydrocarbon saturation	Gas identification	Interval velocity	Acoustic impedance
3	Temperature								–		+						–		
4	Caliper							–					–						
5	SP					–	–						–	+	*				
6	Resistivity	–		–		–	–		+	+	+	+	–		–	*	–		
7	Gamma ray	–	–	+	–	–	–			+				+					
7	Spectral GR	–	–	+	+	–	–	–		+				+					
8	Sonic	+		–		–		+	+	+		*					–	*	*
9	Density	+	–	–	–		–	+	–	+		*					–		*
9	Photoelectric	+	–	–	+														
10	Neutron	+	–	–	–		–			–		*		–			–		
12	Dipmeter					–	–											dip	
13	Image logs	–			–	–	–	+					+			+		dip	

- (Essentially) qualitative use
+ Semi-quantitative and quantitative uses
* Strictly quantitative

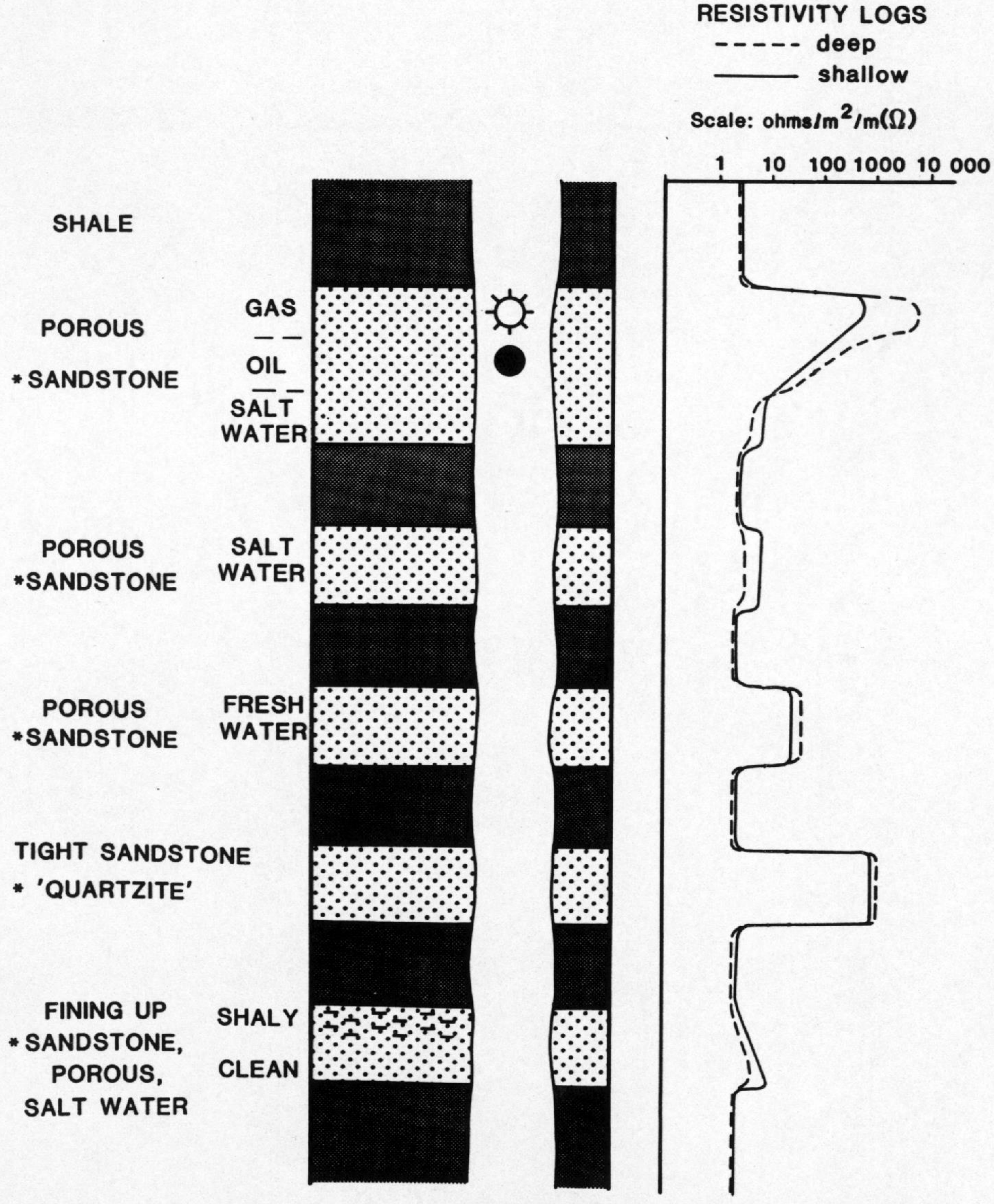
RESISTIVITY LOGS
deep
shallow
Scale: ohms/m²/m(Ω)
1 10 100 1000 10 000
SHALE
POROUS
* SANDSTONE
GAS
OIL
SALT WATER
POROUS
*SANDSTONE
SALT WATER
POROUS
*SANDSTONE
FRESH WATER
TIGHT SANDSTONE
* 'QUARTZITE'
FINING UP
* SANDSTONE,
POROUS,
SALT WATER
SHALY
CLEAN

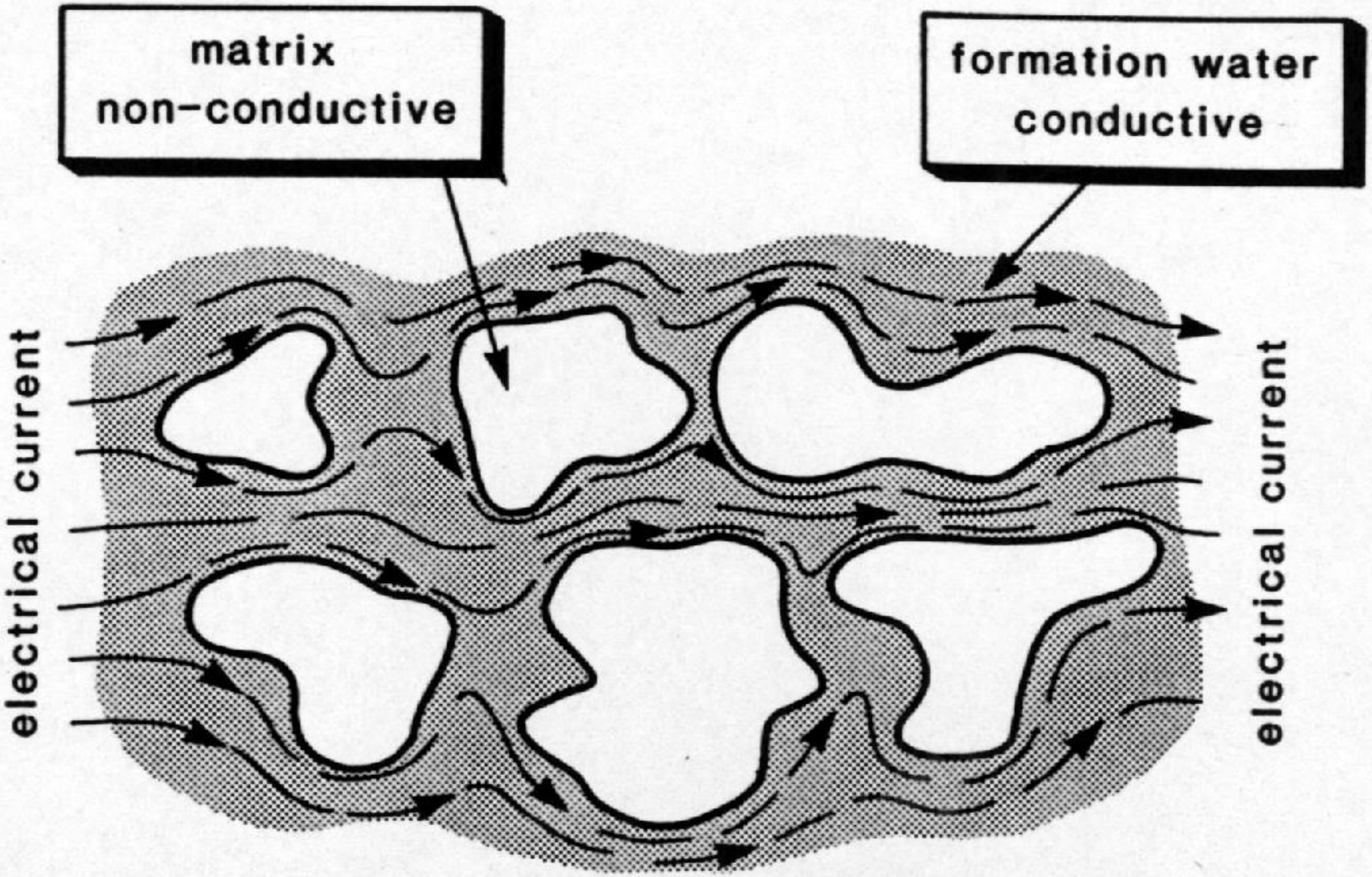

Figure 6.2 Formation conductivity - schematic. The electrical current is restricted to the formation fluids (formation water): the matrix is non-conductive.

Table 6.1 The principal uses of the resistivity and conductivity (induction) logs.

	Discipline	Used for	Knowing
Quantitative	Petrophysics	Fluid saturations: Formation (S_w) Invaded zone (S_{xo}) i.e. detect hydrocarbons	Formation water resistivity (R_w) Mud-filtrate resistivity (R_{mf}) Porosity (ø) (and F) Temperature (T_{fm})
Semi-quantitative and Qualitative	Geology	Textures	Calibration with laboratory samples
		Lithology	Mineral resistivities
		Correlation	
	Sedimentology	Facies, Bedding characteristics	Gross lithologies
	Reservoir geology	Compaction, overpressure and shale porosity	Normal pressure trends
	Geochemistry	Source rock identification Source rock maturation	Sonic and density log values Formation temperature

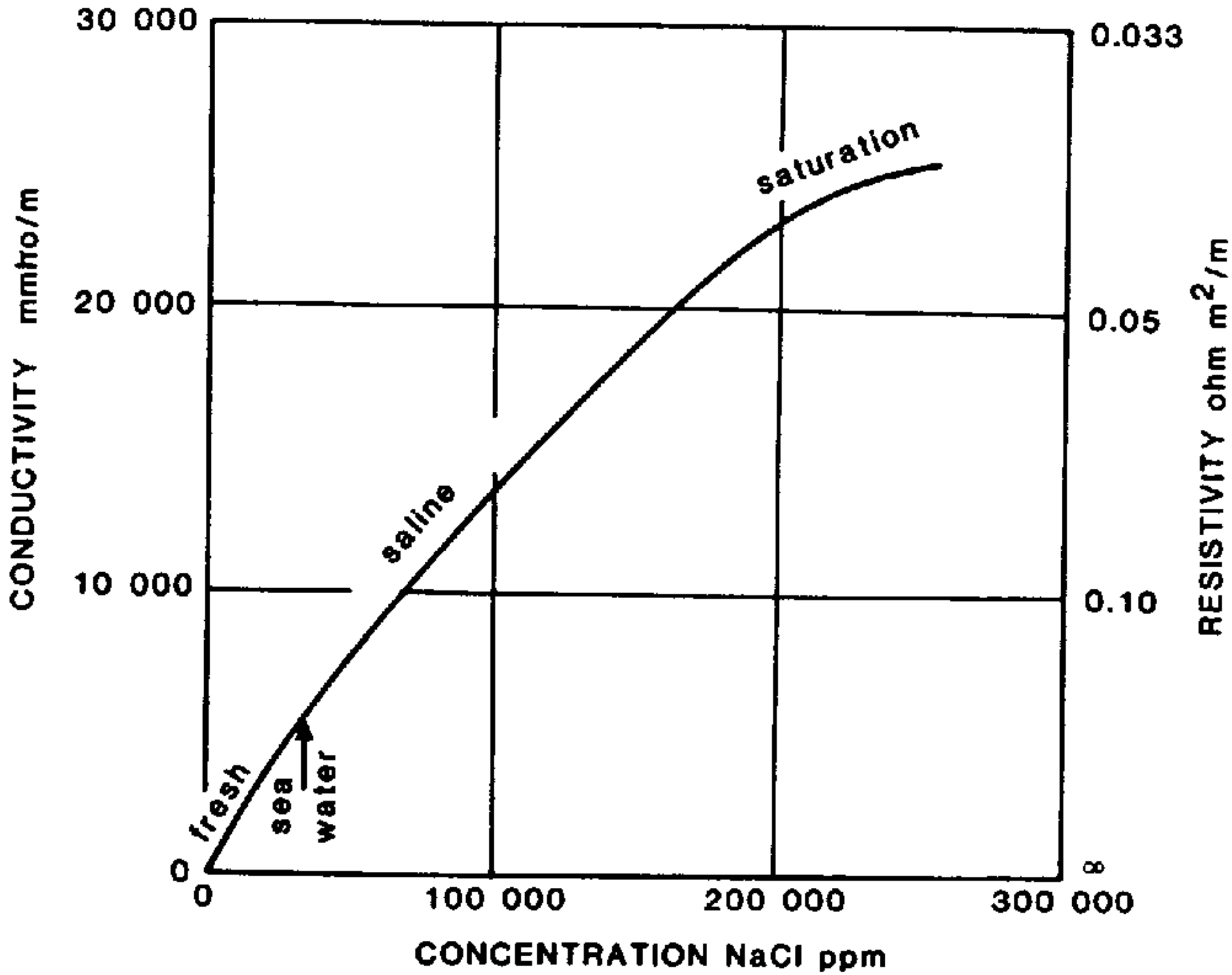

Figure 6.3 Relationship between conductivity (resistivity) and concentration in a salt (NaCl) solution, at 24°C (75°F), modified from Serra, 1979).

Table 6.2 Some typical formation-water salinities.

Origin	Total salinity (ppm)	Type	R_w* ohm m²/m
Sea water	35,000		0.19
Lagunillas, Venezuela	7548†	Fresh	0.77
Woodbine, E. Texas	68,964†	Saline	0.10
Burgan, Kuwait	154,388	Saline	0.053
Simpson sd., Oklahoma	298,497†	Very Saline	(0.04)**

†From Levorsen (1967)

*Approximate R_w (formation-water resistivity) at 24°C (75°F).

**Near the saturation limit.

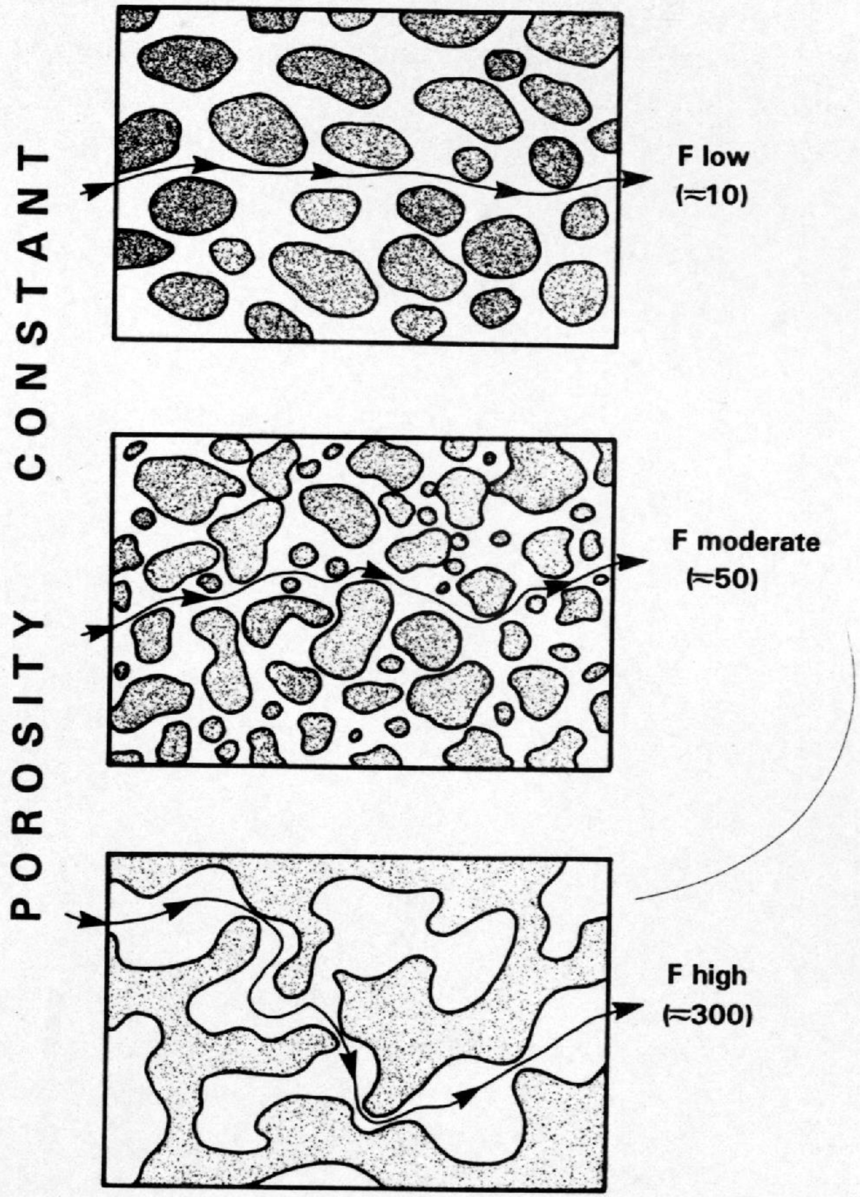

Figure 6.4 Schematic illustration of three formations which have the same porosity but different values of formation resistivity factor, F. The role of the matrix is evident: less at low values of F (top), greater at high values of F (bottom).

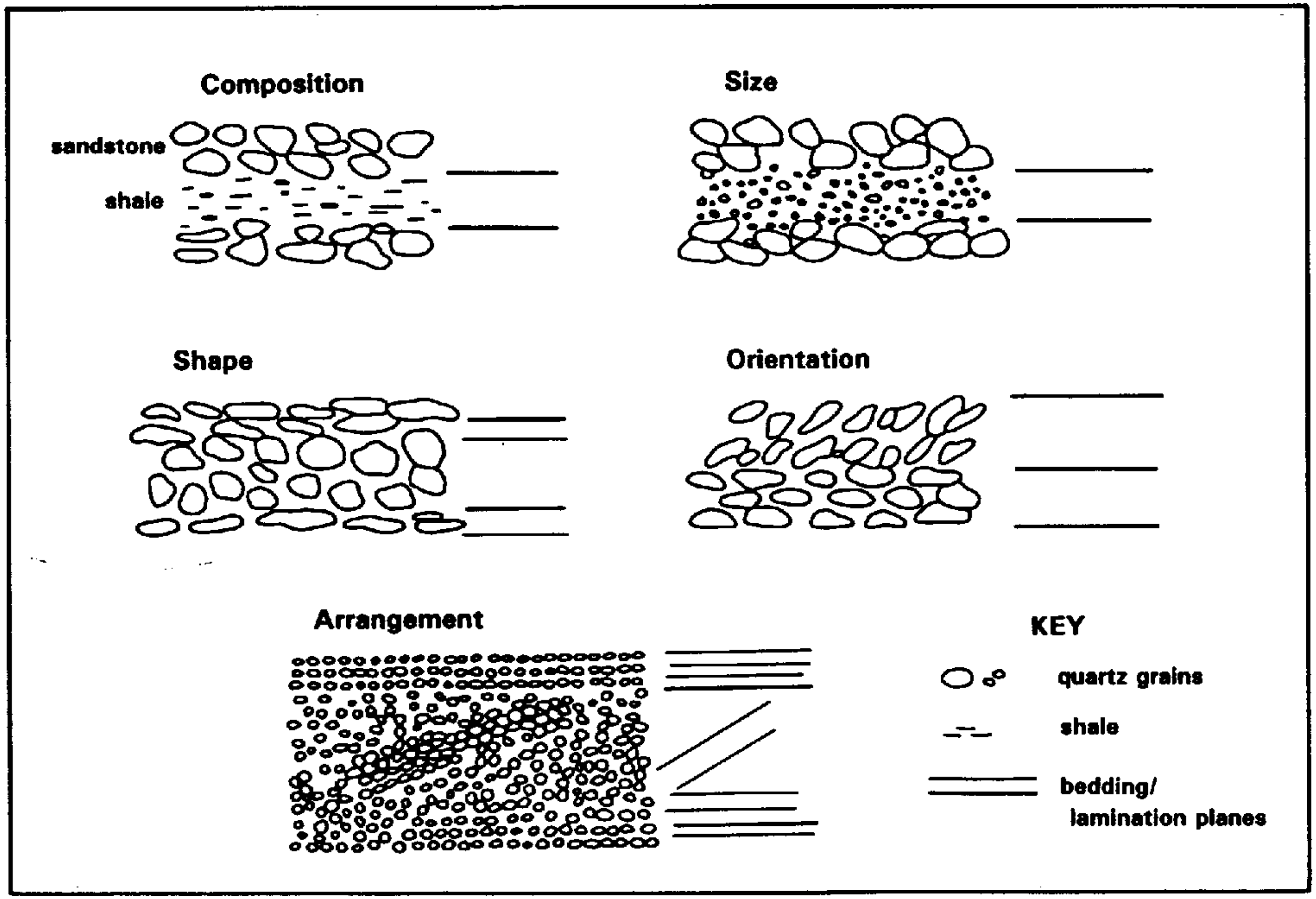

Figure 6.25 The influence of texture on the formation resistivity factor, *F*. Each thin bed or lamina has a different *F* value. This figure should be compared to Figures 6.4 and 6.5 (modified from Nurmi, 1984).

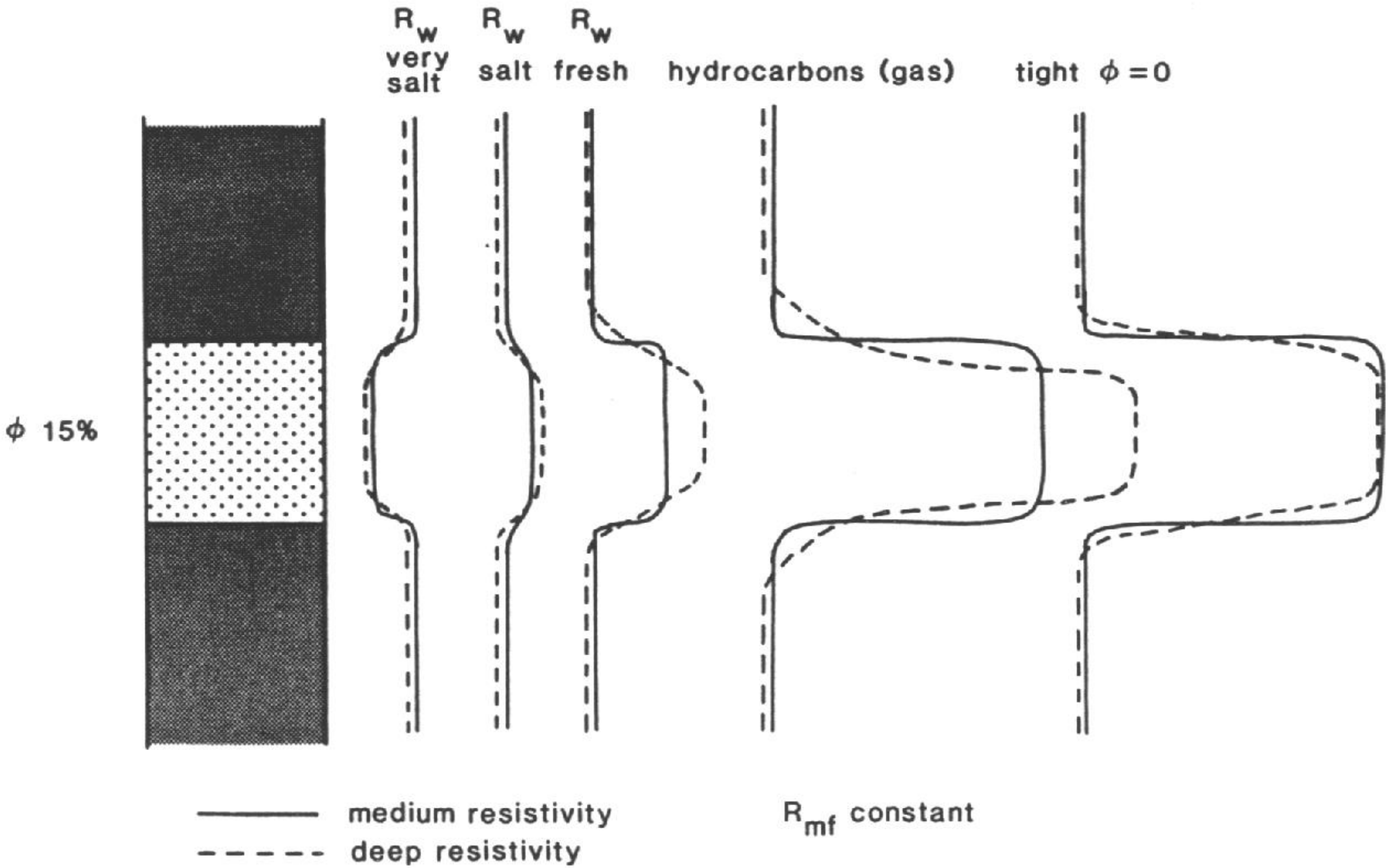

Figure 6.23 Schematic illustration of the behaviour of resistivity logs over the same reservoir bed but with different fluids and, in the last case, no porosity.

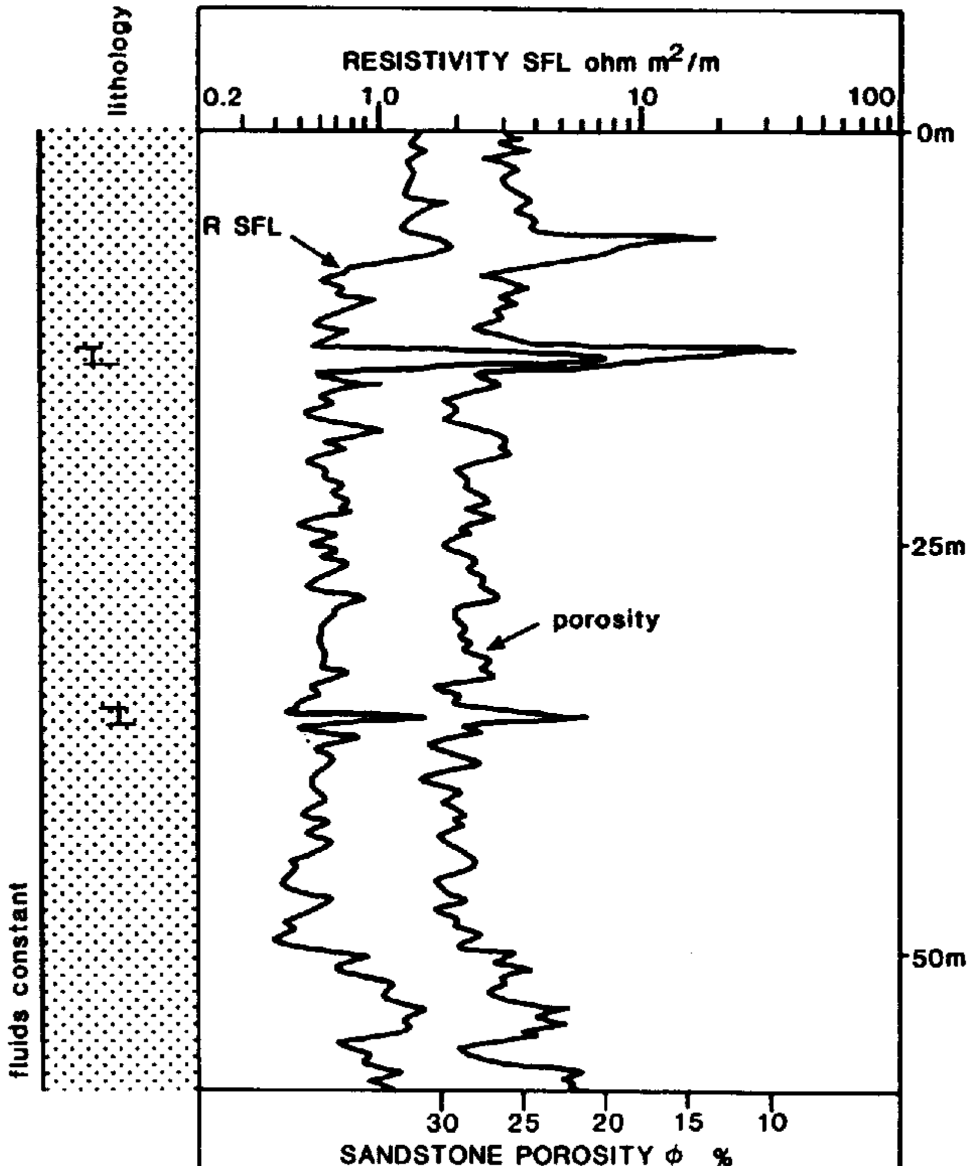

Figure 6.24 The close relationship between resistivity and porosity in a water-bearing sandstone. Resistivity from spherically focused log, SFL: porosity is log-derived.

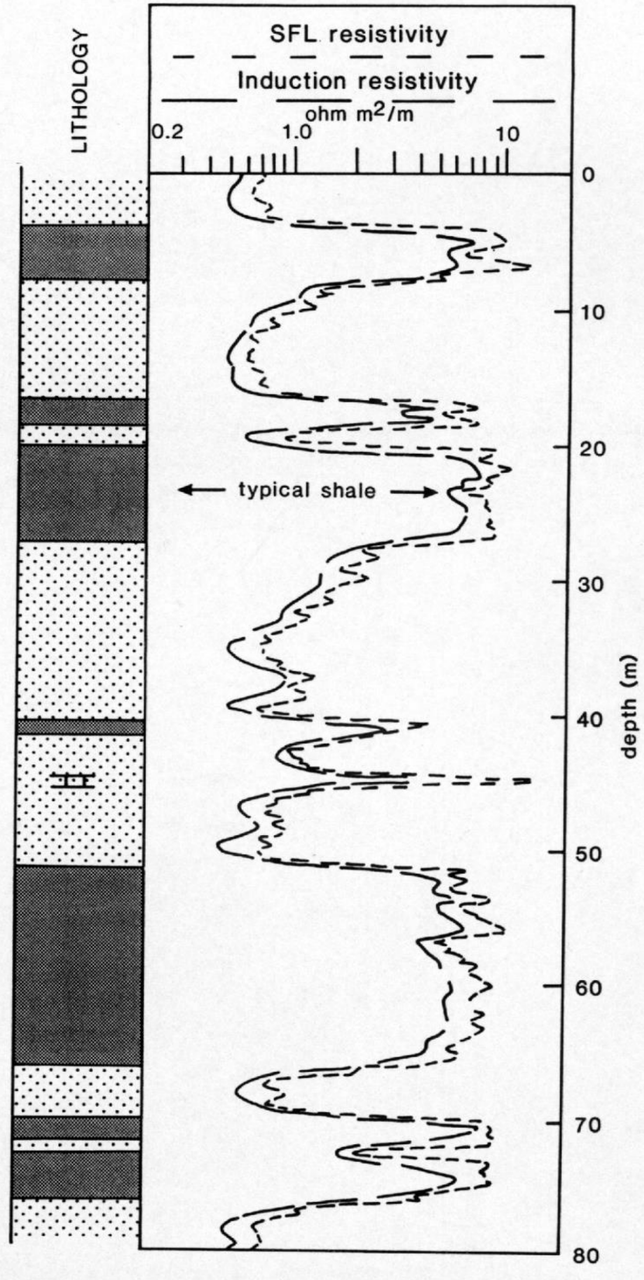

Figure 6.27 Shale intervals shown on the resistivity logs. In most sand-shale sequences, shales tend to have a constant, typical value.

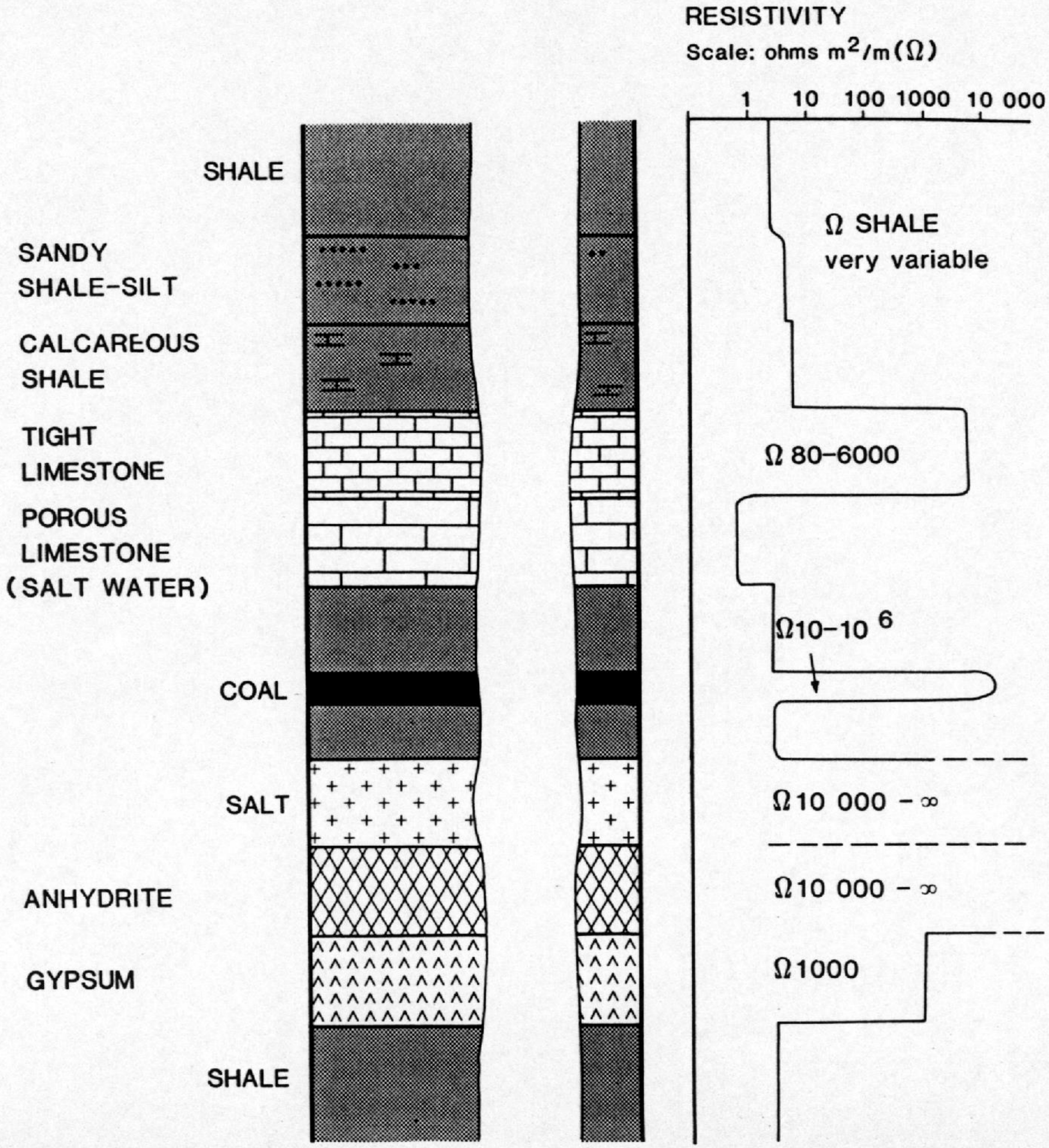

Figure 6.28 Responses on a deep resistivity log of some minerals and some typical, distinctive lithologies. To these mineral values should be added the following fluid values: pure, fresh water (26.7°C) = α , salt-saturated water (26.7°C) = 0.032Ω , methane = α .

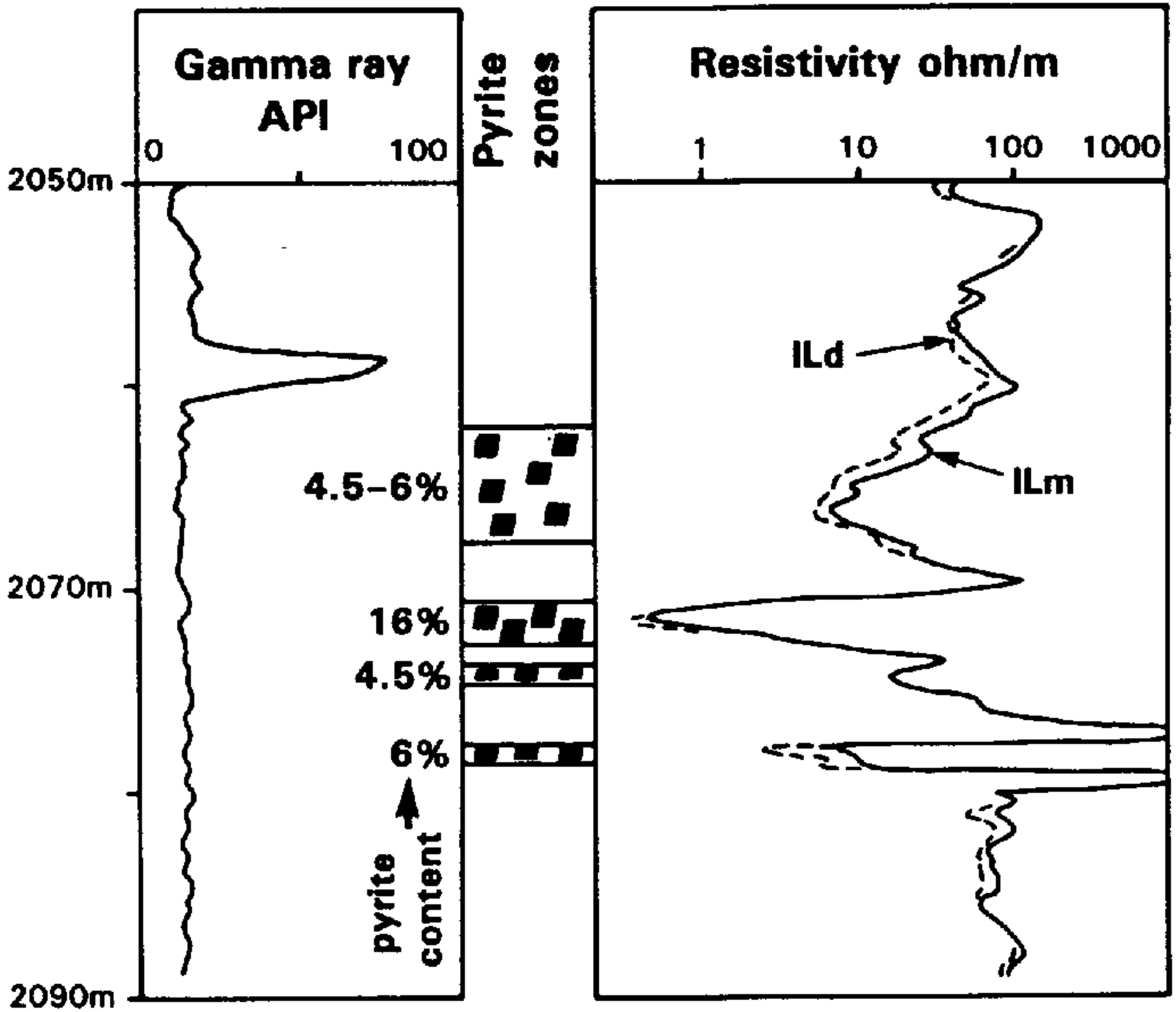

Figure 6.29 The effect of pyrite on induction logs. At high concentrations the electrical conductivity of pyrite is seen and log resistivity values are significantly lowered (re-drawn, modified from Theys, 1991, attributed to Clavier *et al.*, 1976).

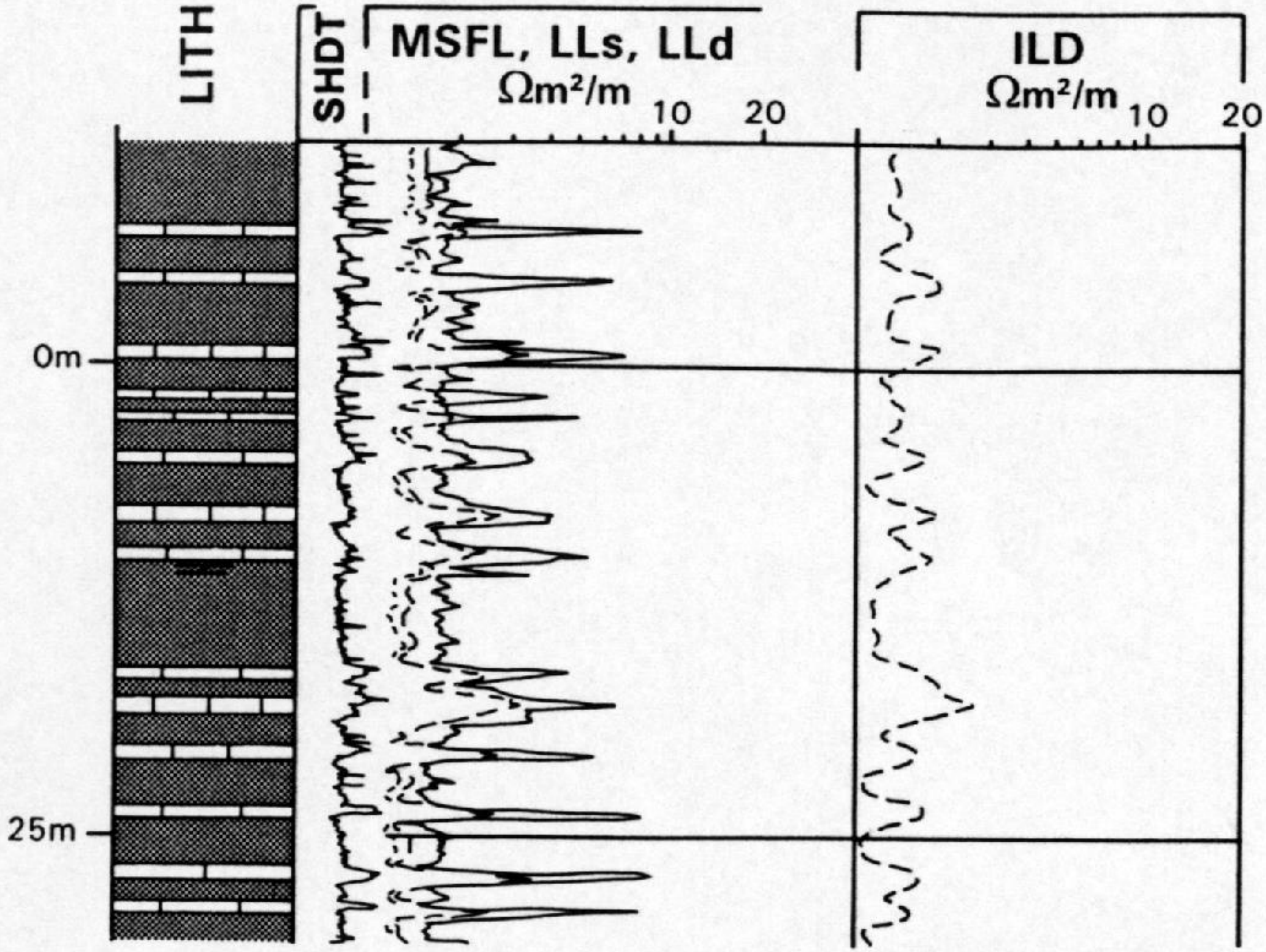

Figure 6.30 Siderite stringers in a shale sequence as seen on resistivity logs. The SHDT dipmeter curve (2.5mm sampling) shows that these are very thin, often concretionary layers.

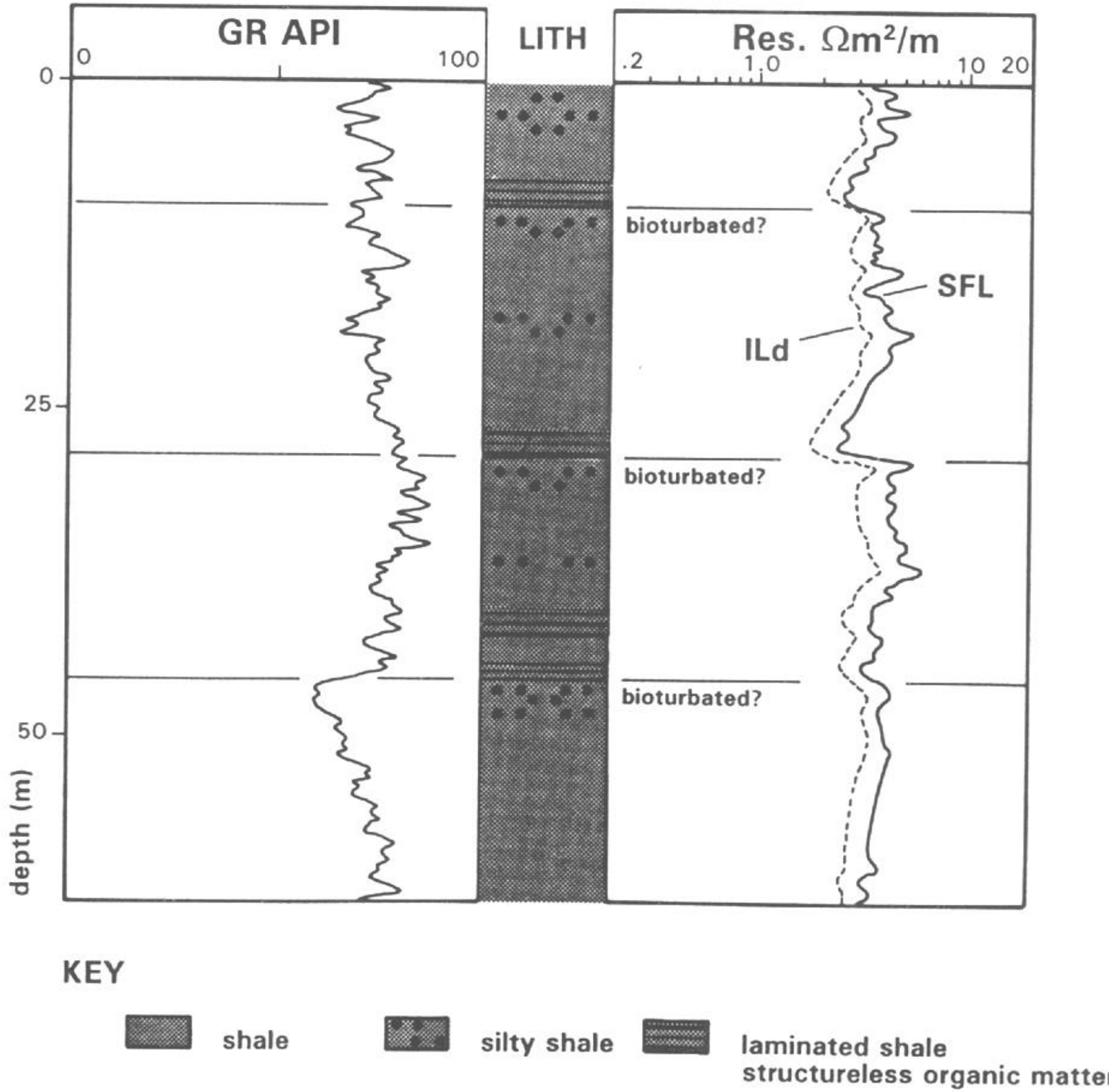

Figure 6.31 Subtle textural and compositional variations in shallow marine shales indicated on the resistivity logs.

Compositional changes are noted in the organic matter content and in the amount of silt. Textural variation is seen in the fine lamination of the organic rich shales which causes distinctive, low resistivities. Note the separation between the shallow (SFL) and deep (ILd) devices (*see* text).

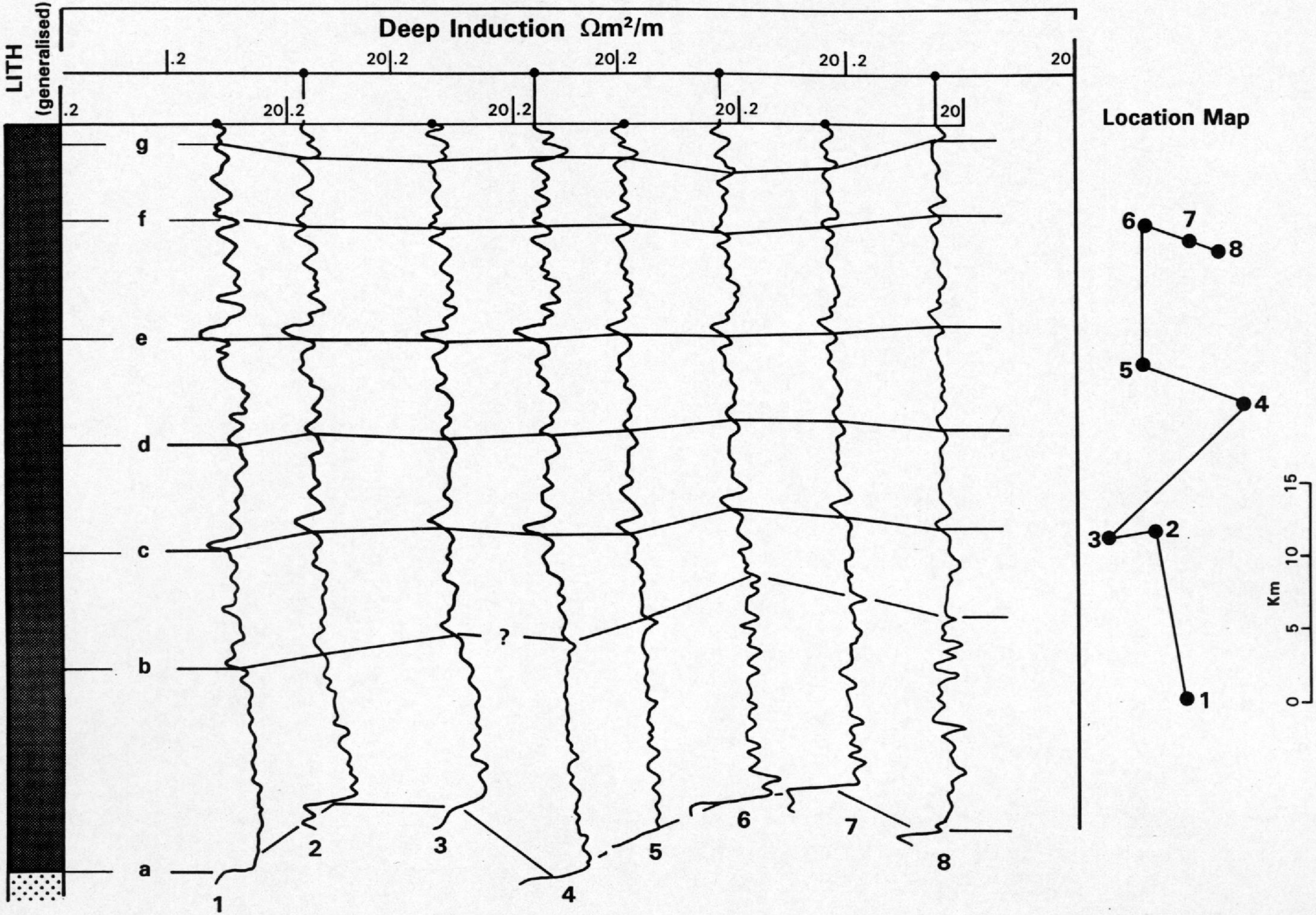

Figure 6.32 Correlation using deep induction logs (resistivity plots). The interval is one of thick, seemingly characterless, marine shales. The logs show persistent, subtle changes which allow excellent correlation over a distance of 30km.

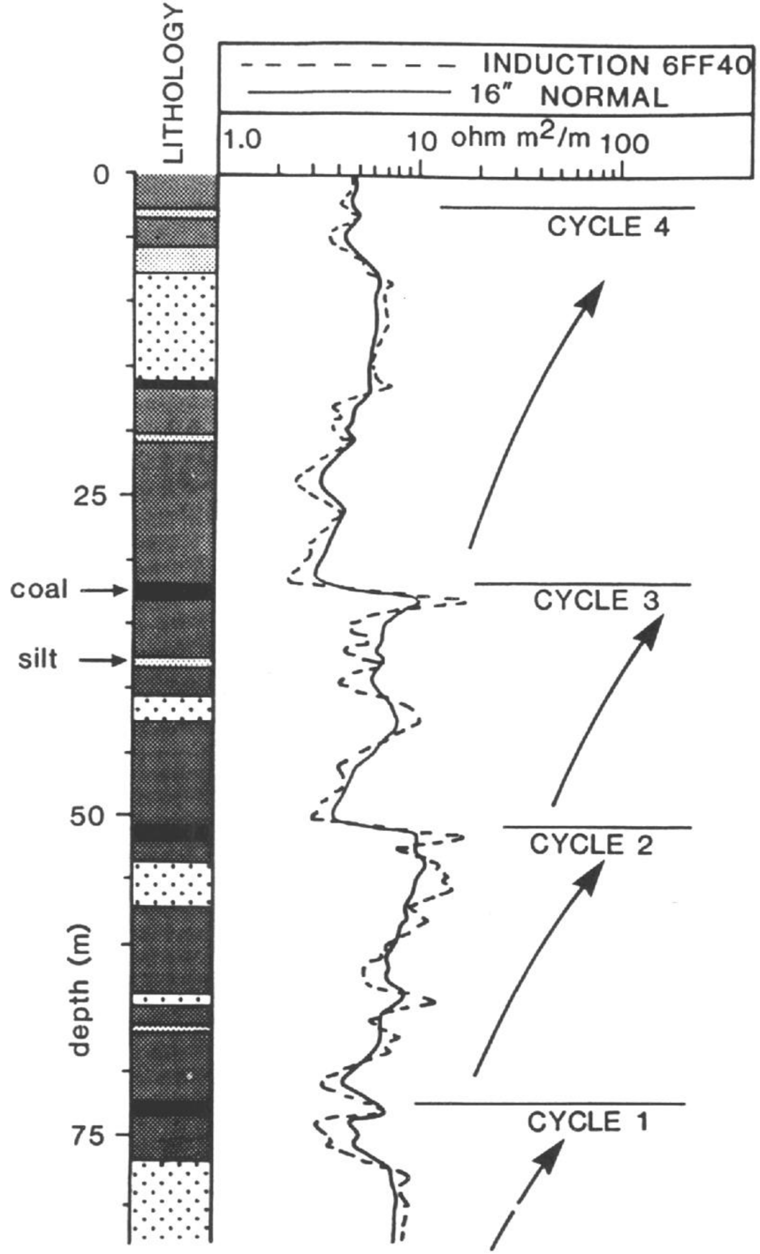

Figure 6.33 Resistivity logs showing small-scale deltaic cycles. The resistivity varies with changes in the sand-shale percentages.

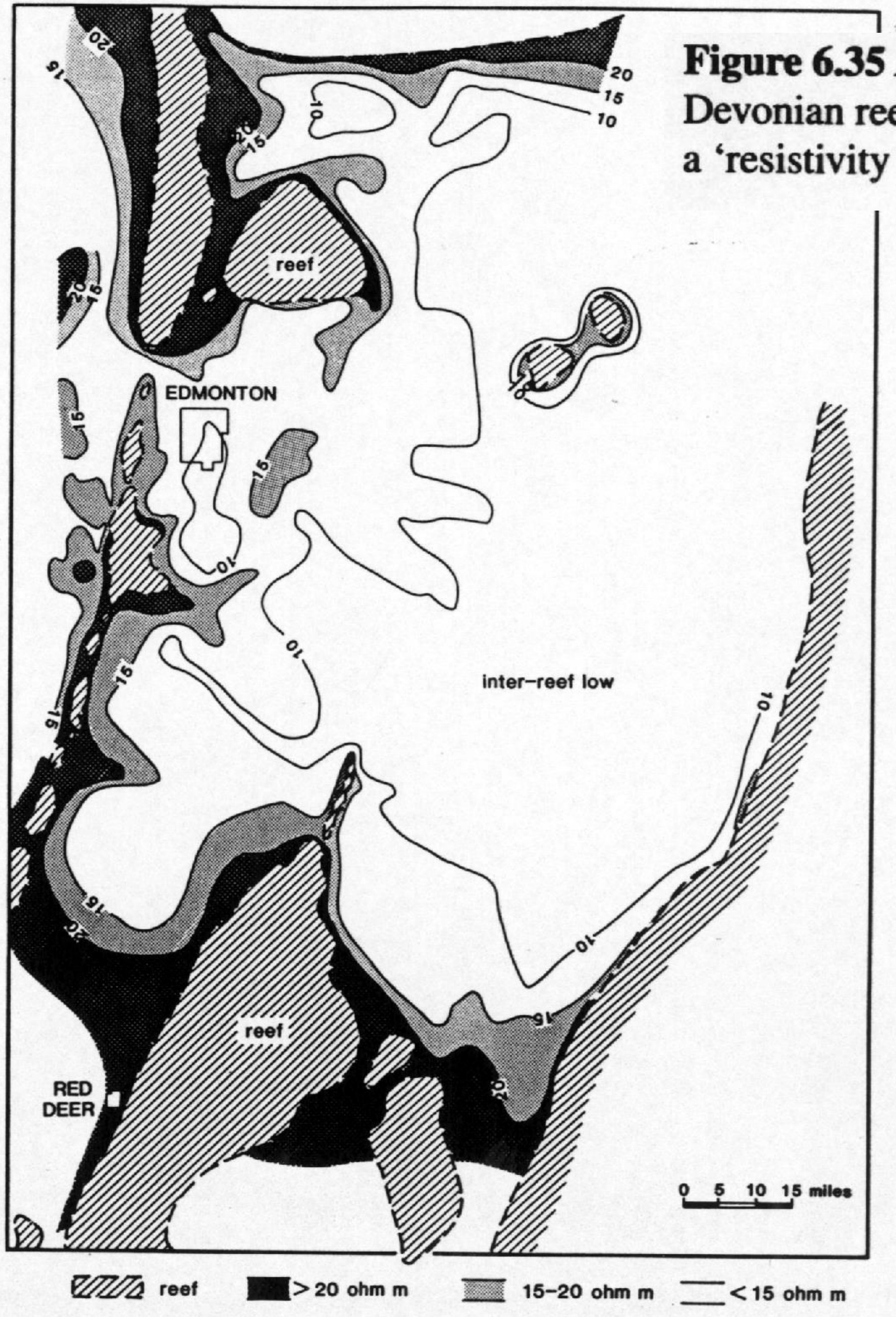

Figure 6.35 A resistivity map of the middle and lower Ireton. Devonian reef complex, Canada. The reefs are surrounded by a 'resistivity gradient'. (Redrawn from McCrossan, 1961).

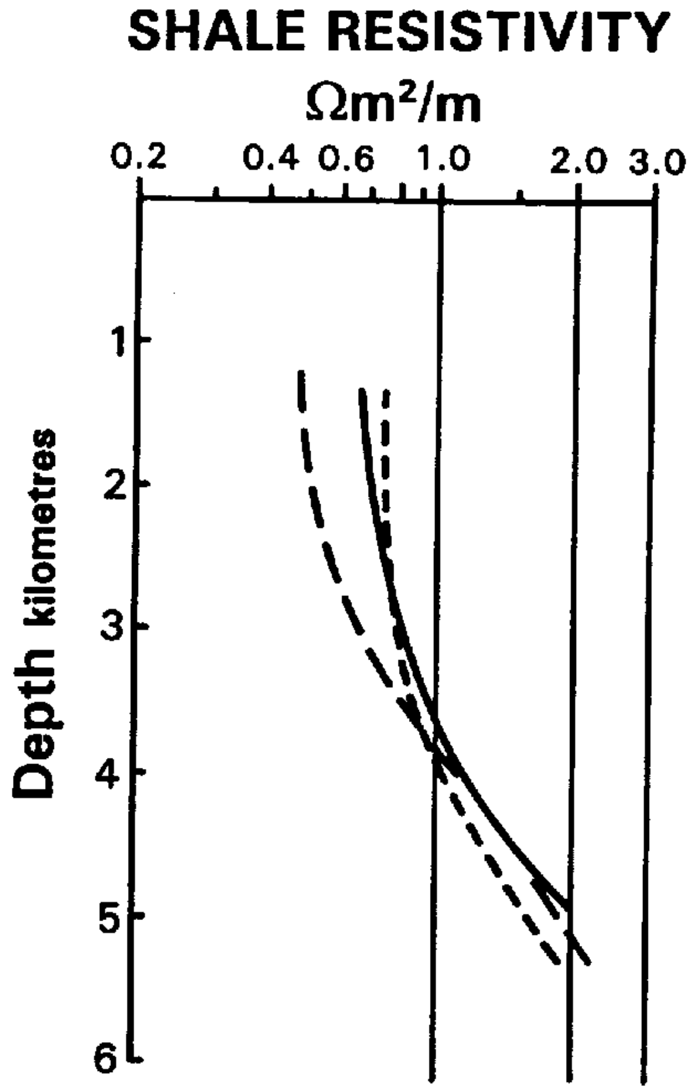

Figure 6.36 Shale resistivity trends with depth. The example shows normal compaction trends from the Gulf Coast 1, Oligocene-Miocene; 2, 3, Miocene, Louisiana. (Redrawn from Magara, 1978, after Hottman and Johnson, 1965).

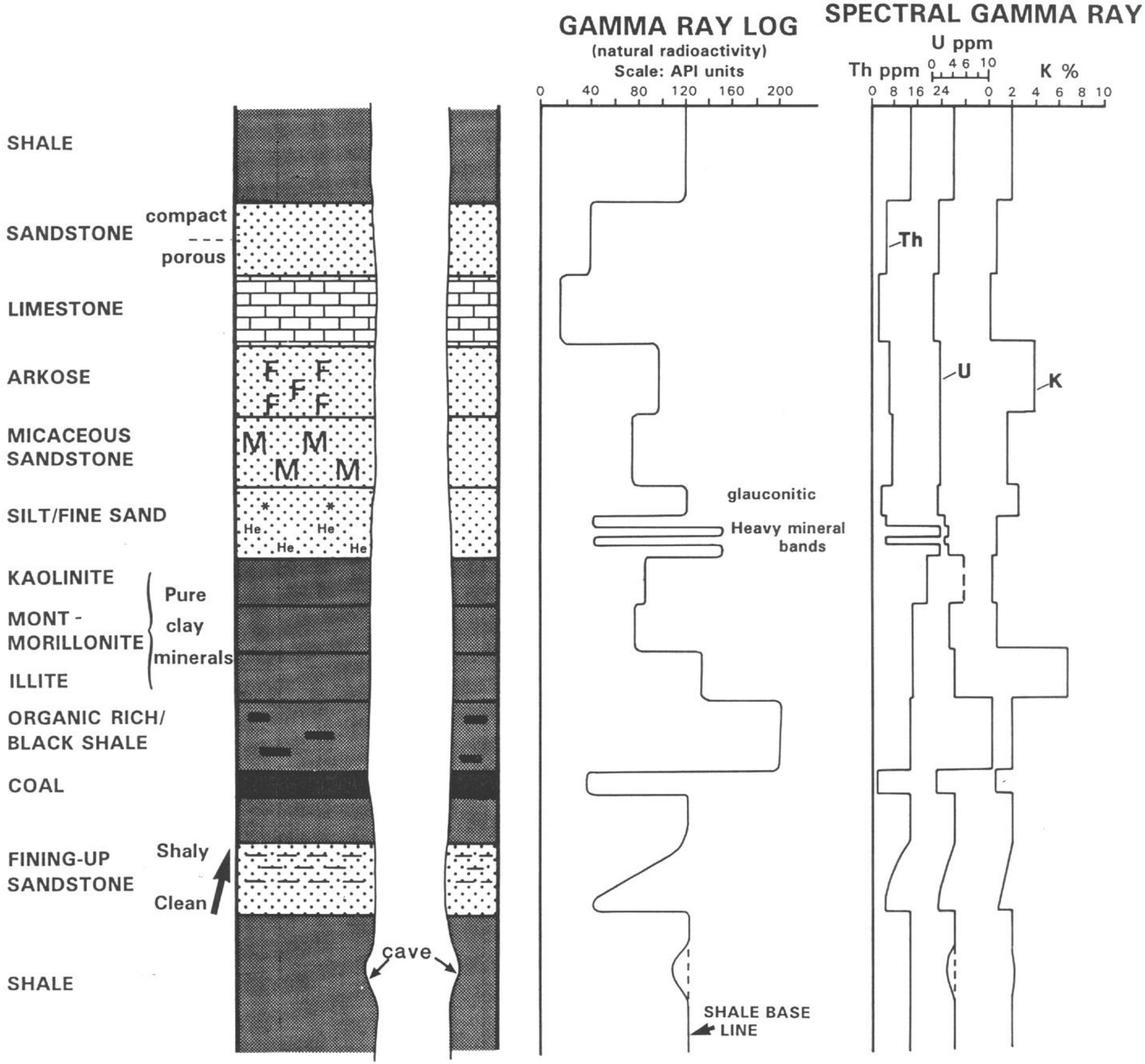
GAMMA RAY LOG
(natural radioactivity)
Scale: API units
0 40 80 120 160 200
SPECTRAL GAMMA RAY
U ppm
0 4 6 10
Th ppm
0 8 16 24
K %
0 2 4 6 8 10
SHALE
SANDSTONE
compact
porous
LIMESTONE
ARKOSE
MICACEOUS SANDSTONE
SILT/FINE SAND
KAOLINITE
MONT - MORILLONITE
ILLITE
Pure clay minerals
ORGANIC RICH/ BLACK SHALE
COAL
FINING-UP SANDSTONE
Shaly
Clean
SHALE
cave
glauconitic
Heavy mineral bands
Th
U
K
SHALE BASE LINE

Table 7.1(a) Principal uses of the gamma ray log.

	Discipline	Used for	Knowing
Quantitative	Petrophysics	Shale volume (*Vsh*)	gamma ray (max) gamma ray (min)
Qualitative	Geology	Shale (shaliness)	gamma ray (max) gamma ray (min)
		Lithology	typical radioactivity values
		Mineral identification	Mineral radioactivity
	Sedimentology	Facies	Clay/grain size relationship
	Sequence Stratigraphy	Parasequence & condensed sequence identification	Clay/grain size & organic matter/radioactivity relationships
	Stratigraphy	correlation	–
		Unconformity identification	–

A. AVERAGE INVESTIGATION DEPTH

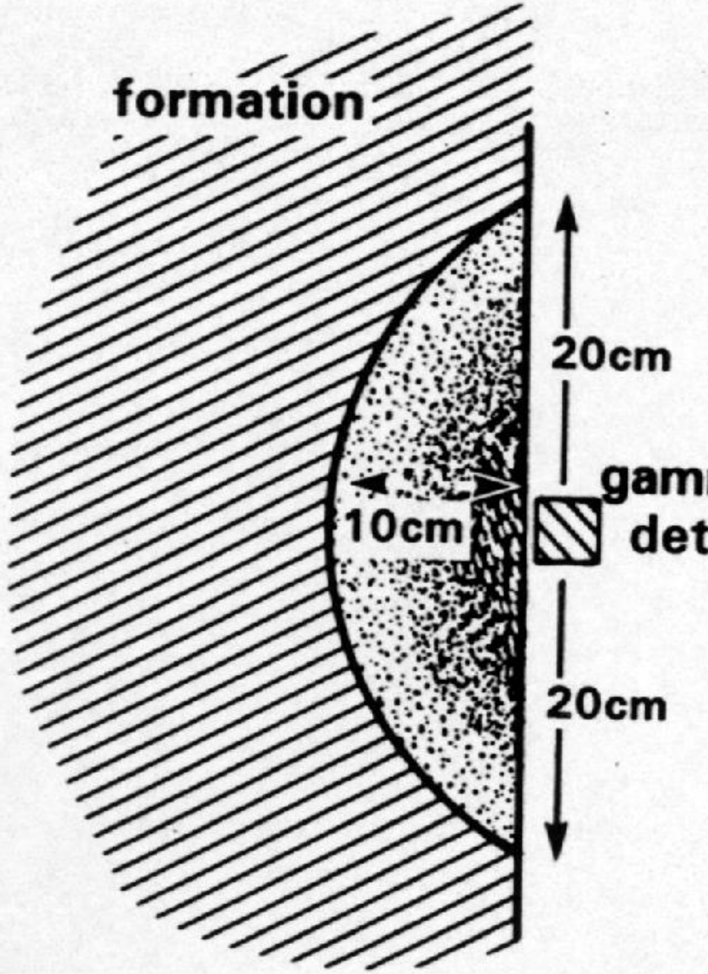

Resolution:

vertical 40cm

depth 10cm

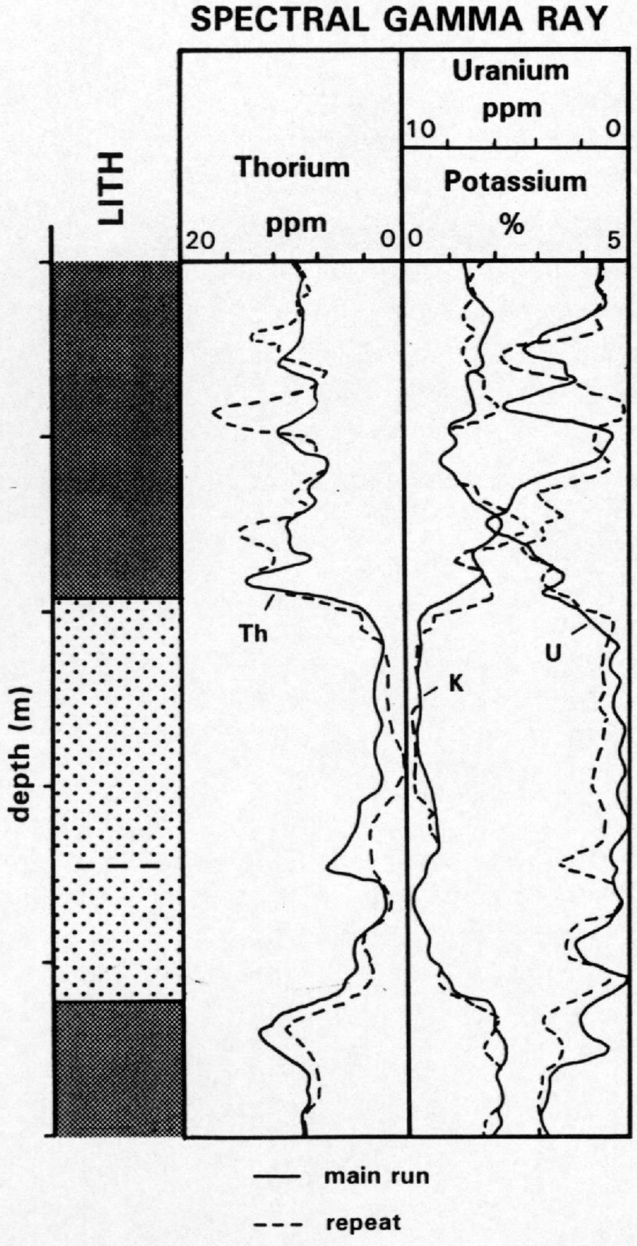

Figure 7.9 Repeatability of the spectral gamma ray. Precise repeatability is generally poor but it should be noted that the quantities being detected are very small.

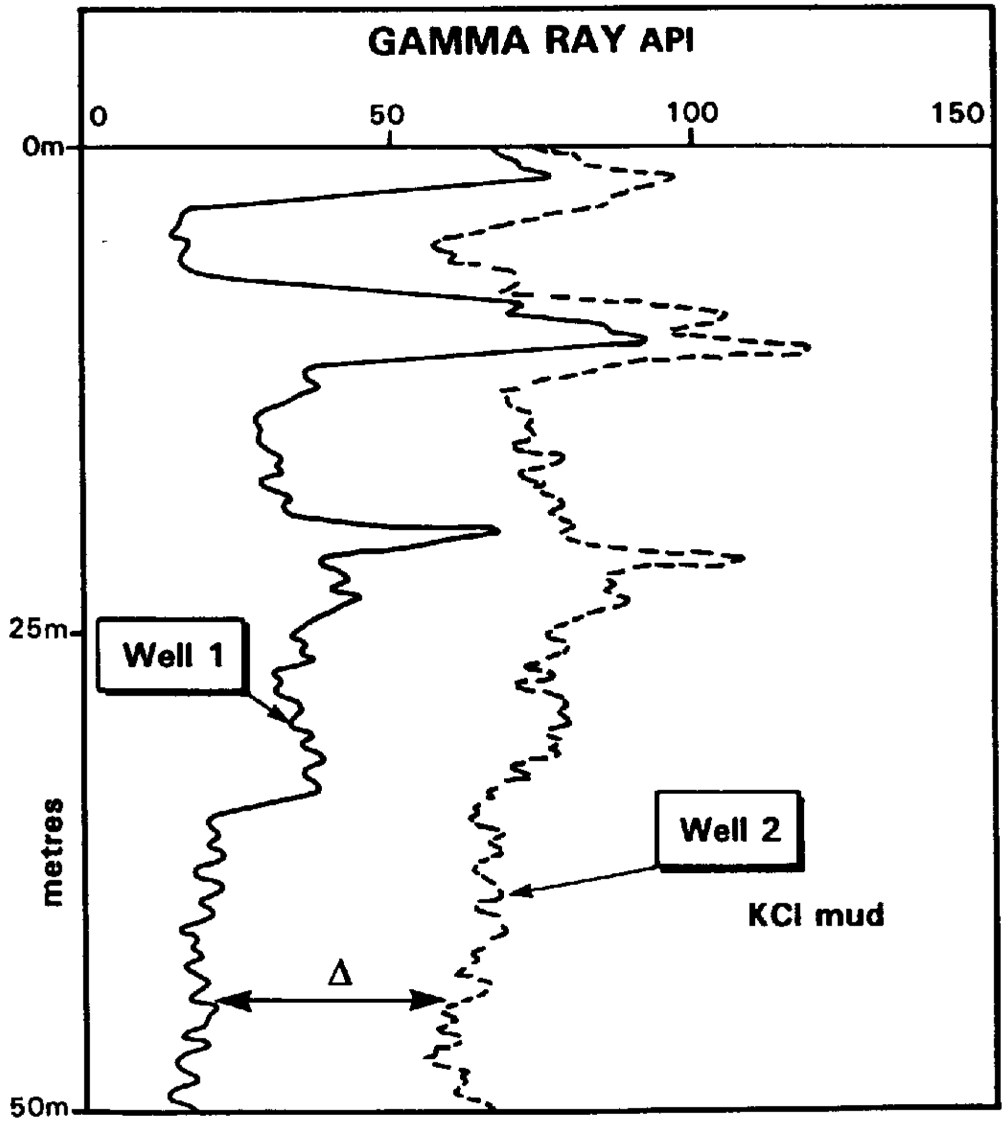

Figure 7.10 The effect of KCl in the drilling mud on gamma ray values. Well 1, with ordinary mud, well 2 with KCl mud. The formation values should be the same. Δ, is the difference created by the KCl content. The wells are 3km apart.

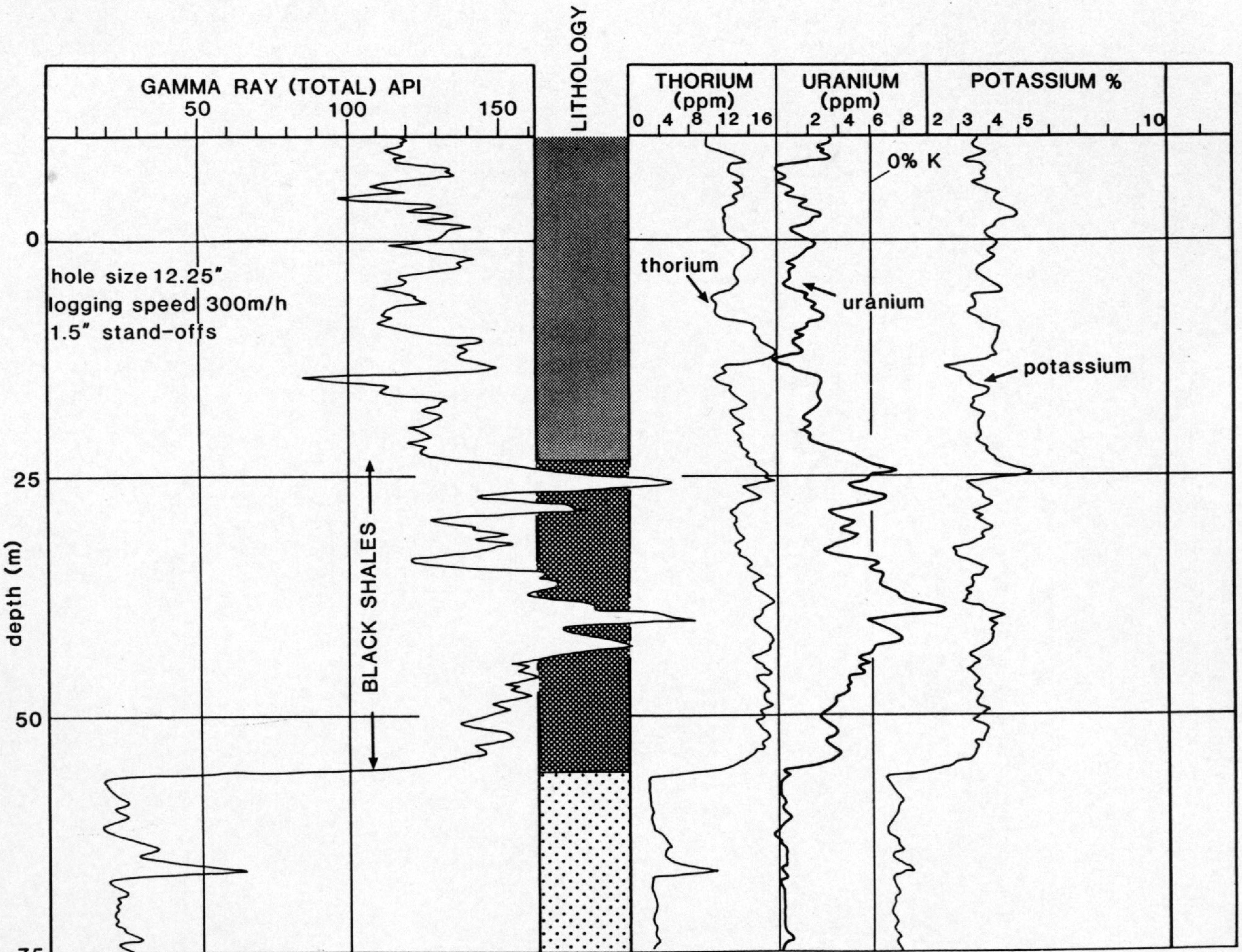

Figure 7.11 'Black shale' radioactivity. A spectral gamma ray log over the Upper Jurassic black shales of the North Sea showing the high uranium contribution.

Table 7.12 Thorium-bearing heavy minerals (Serra *et al.*, 1980).

	Composition	**ThO_2 content (%)**
Thorite	Th, Si, O_4	25–63
Monazite	Ce, Y, La, PO_4	4–12
Zircon	Zr, Si, O_4	less than 1
	Uranium ppm	**Thorium pm**
Zircon	300–3000	100–2500
Sphene	100–700	100–600
Epidote	20–50	50–500
Apatite	5–150	2–150

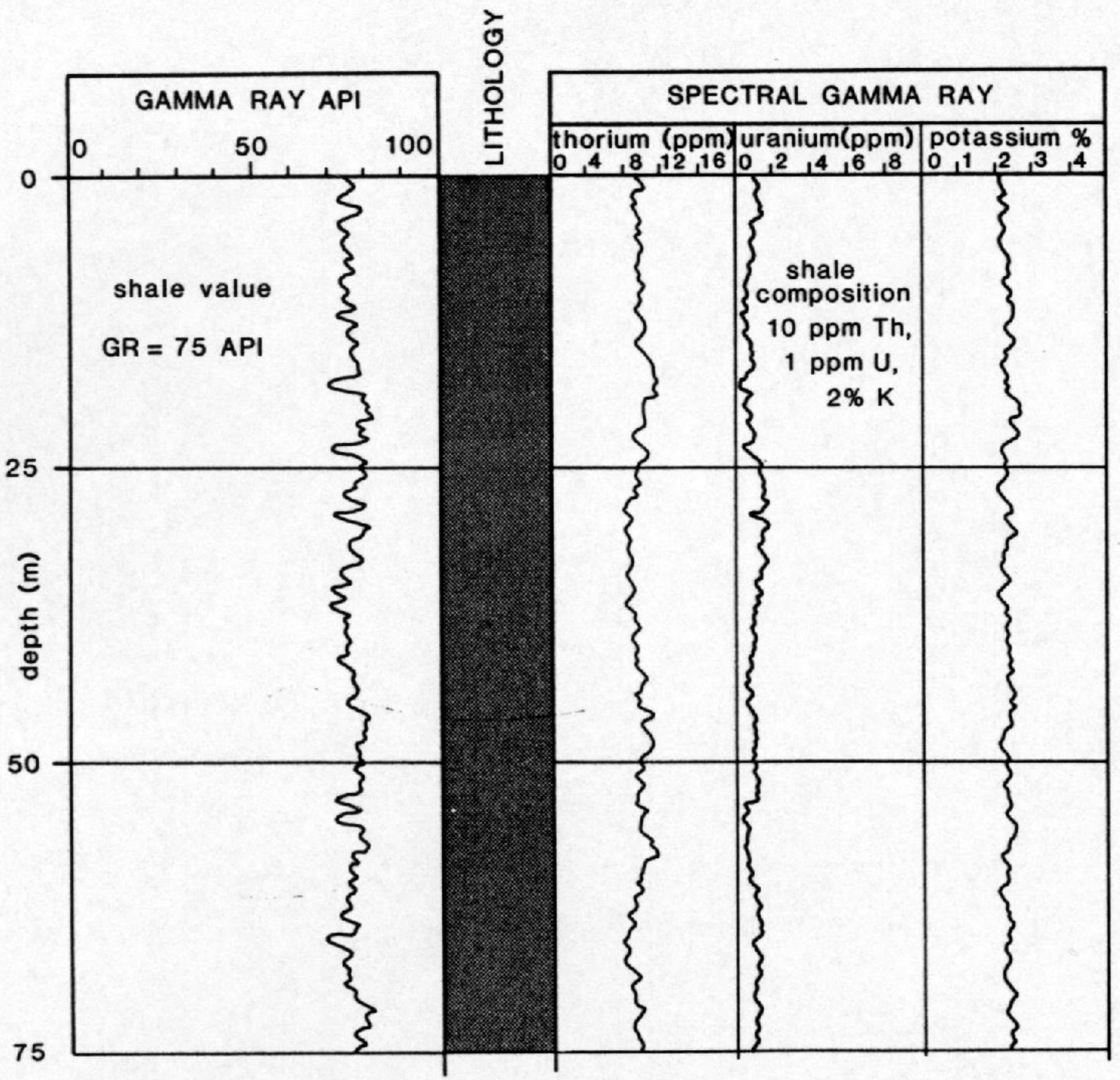

Figure 7.13 A typical shale interval analysed by a spectral gamma ray tool. The log shows the individual contributions of thorium, potassium and uranium to the overall radioactivity.

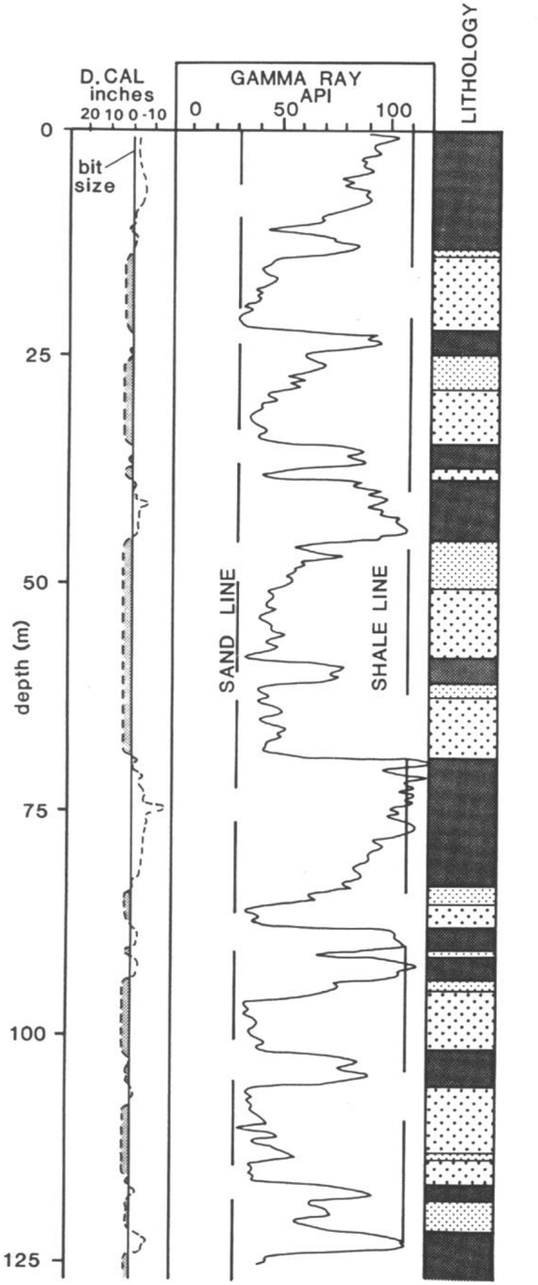

Figure 7.14 Sand line and shale line defined on a gamma ray log. These 'baselines' are for the quantitative use of the log, and may be reasonably constant in any one zone.

Table 7.15 Potassium content of some common detrital materials (from Serra, 1979; Edmundson *et al.*, 1979; Dresser Atlas, 1983; Schlumberger, 1985).

	Mineral species	% potassium by weight	Average %	Gamma ray value (API)
Micas	Glauconite*	3.2 –5.8	4.5	75† – 90†
	Muscovite	7.9 – 9.8	9.8	140† – 270
	Botite	6.2 – 10.1	8.7	90† – 275
Feldspars	Microline	10.9 – 16	16	220 – 280†
	Orthoclase	11.8 – 14	14	220 – 280†

*Detrital or authigenic

†For 8in hole, 1.2g/cm³ mud, 3⅝in NaI scintillator

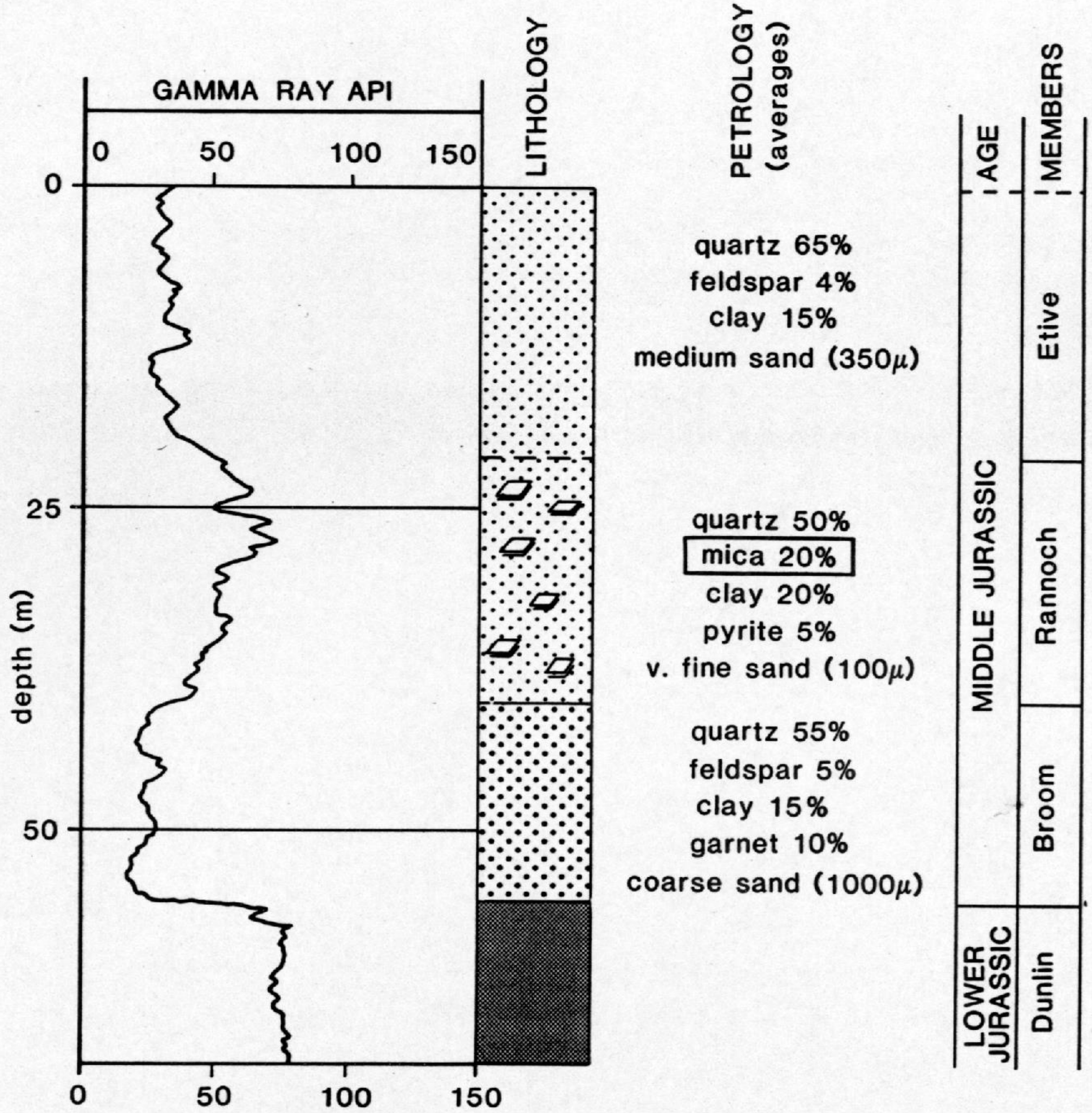

Figure 7.17 Radioactive sand, the 'mica sands' of the North Sea Jurassic. They are fine-grained shallow marine sandstones with perhaps 20% clay but 15 – 30% mica, mainly muscovite, which causes the radioactivity.

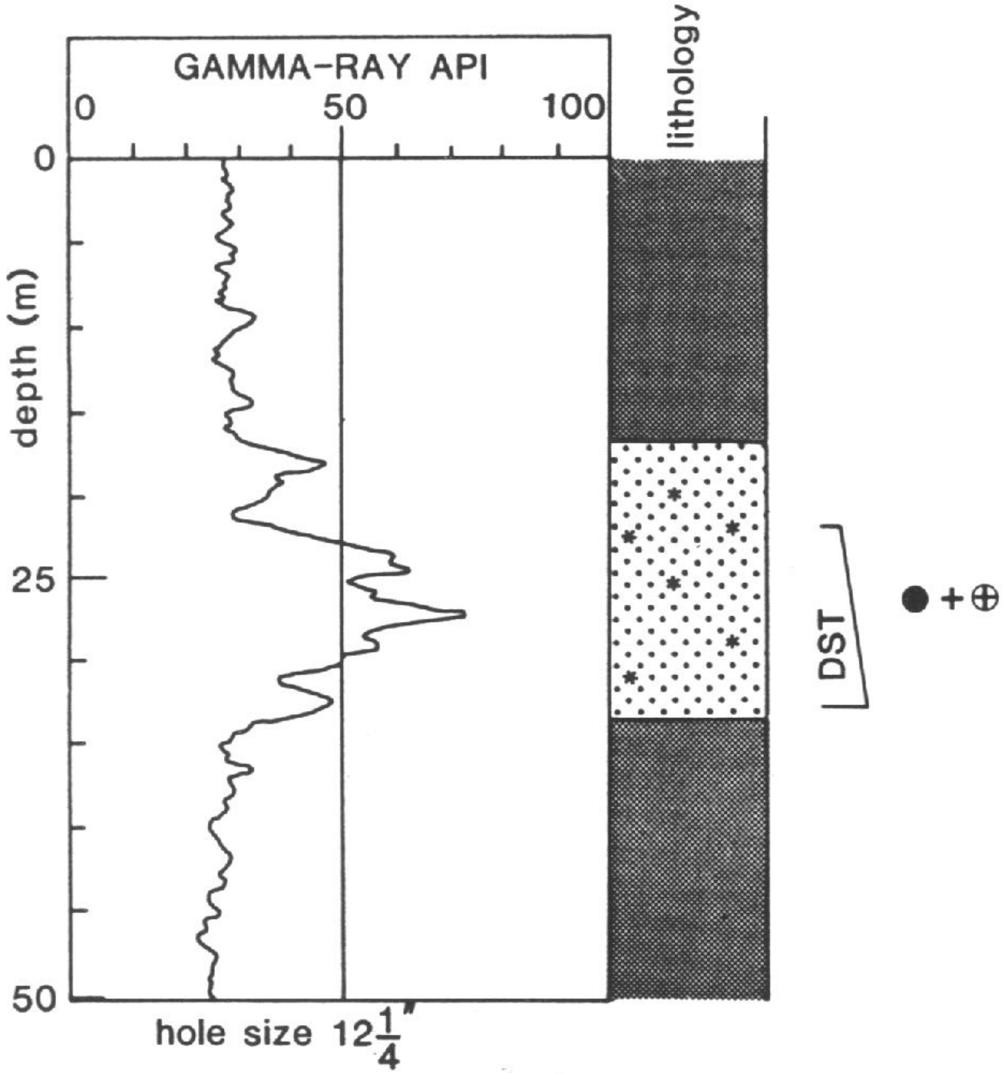

Figure 7.18 Glauconite causing radioactivity in a sandstone interval. Silty sands envelop this marine, glauconite-rich sand giving the sands higher gamma ray log values than the shales. An oil flow confirms the reservoir characteristics. DST = Drill Stem Test. *Glauconite.

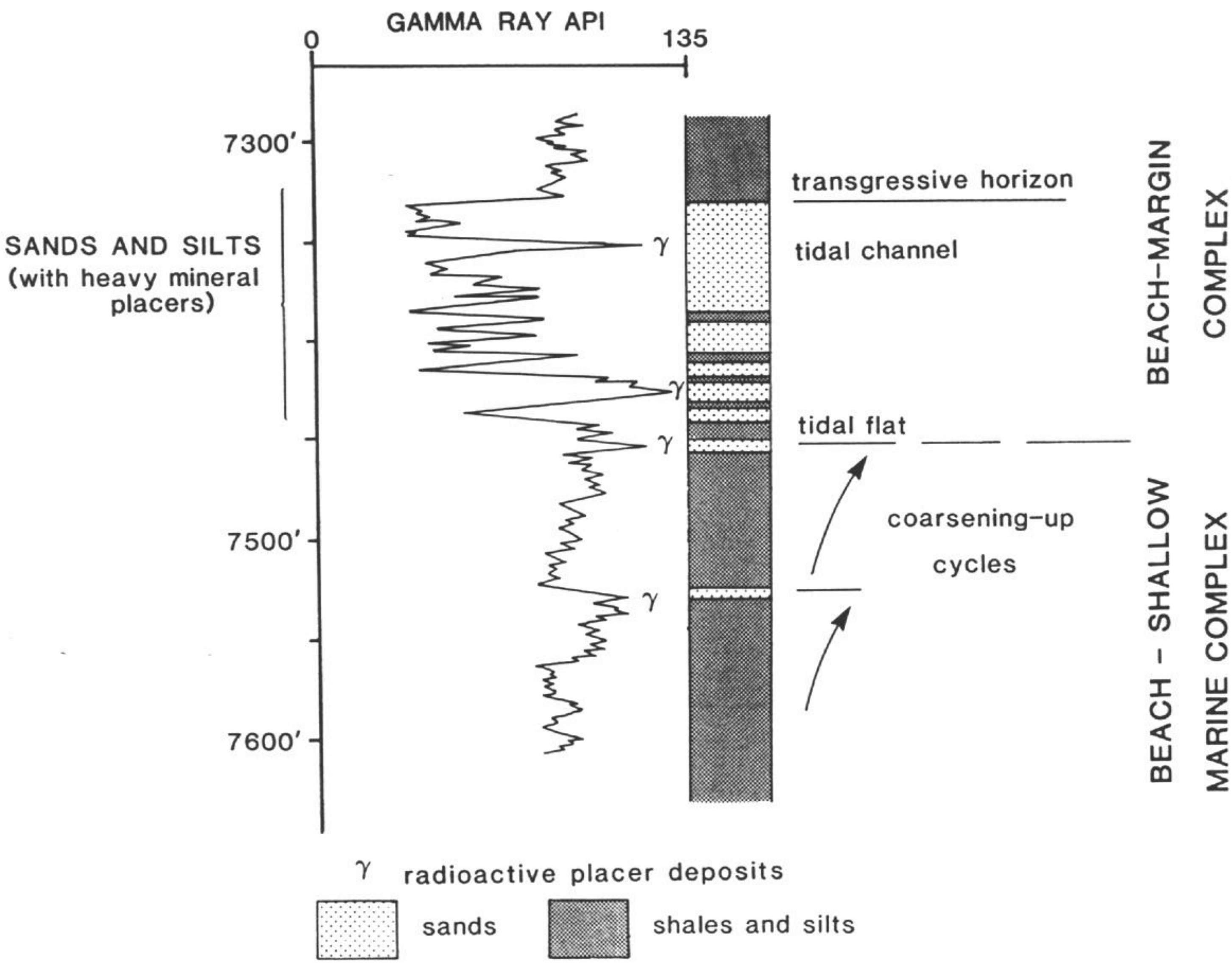

Figure 7.19 Heavy mineral concentrations (placer deposits) causing a spiky gamma ray log. Shales have lower gamma ray values than the heavy mineral deposits (Nigeria). (Re-drawn from Serra, 1974).

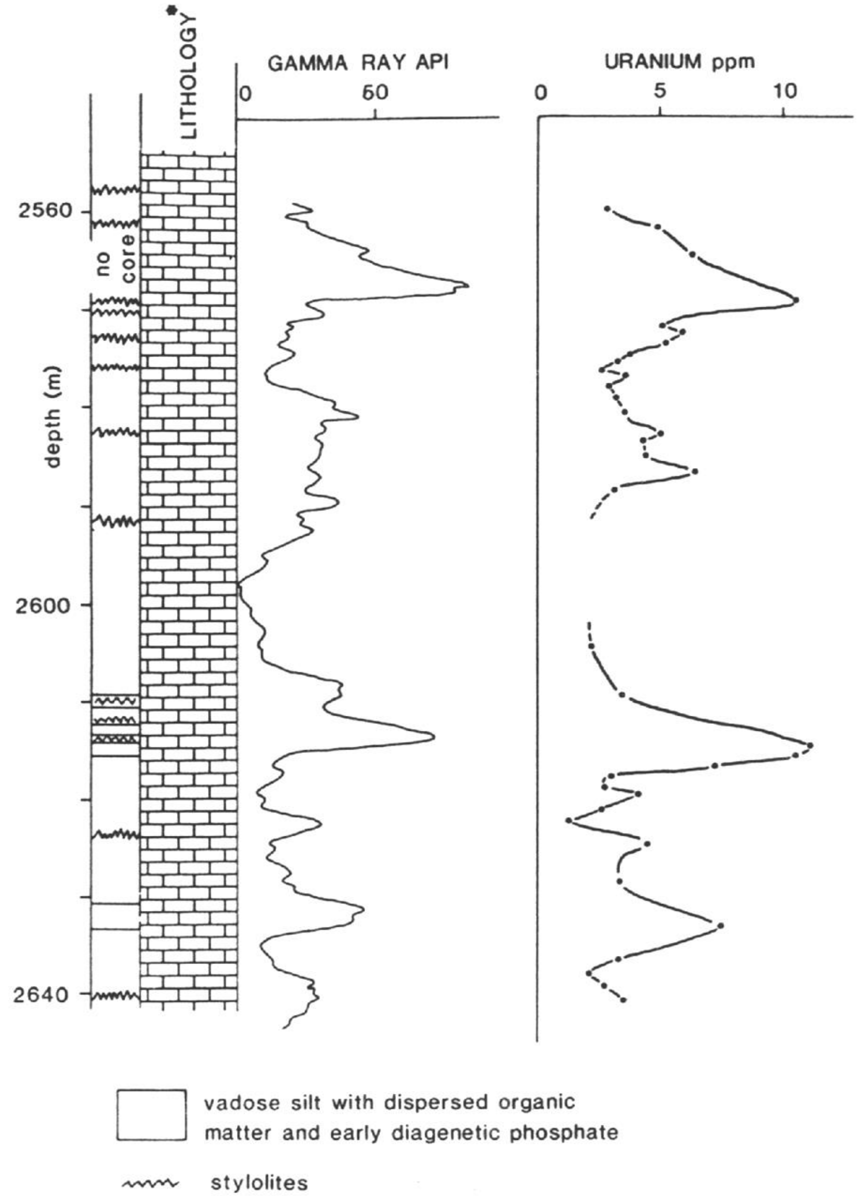

Figure 7.20 Radioactivity of Ypresian (Eocene) Limestones, Tunisia, related to uranium concentrations. The uranium is associated with early diagenesis, organic matter and phosphatic concentrations. (Re-drawn from Hassan, 1973).

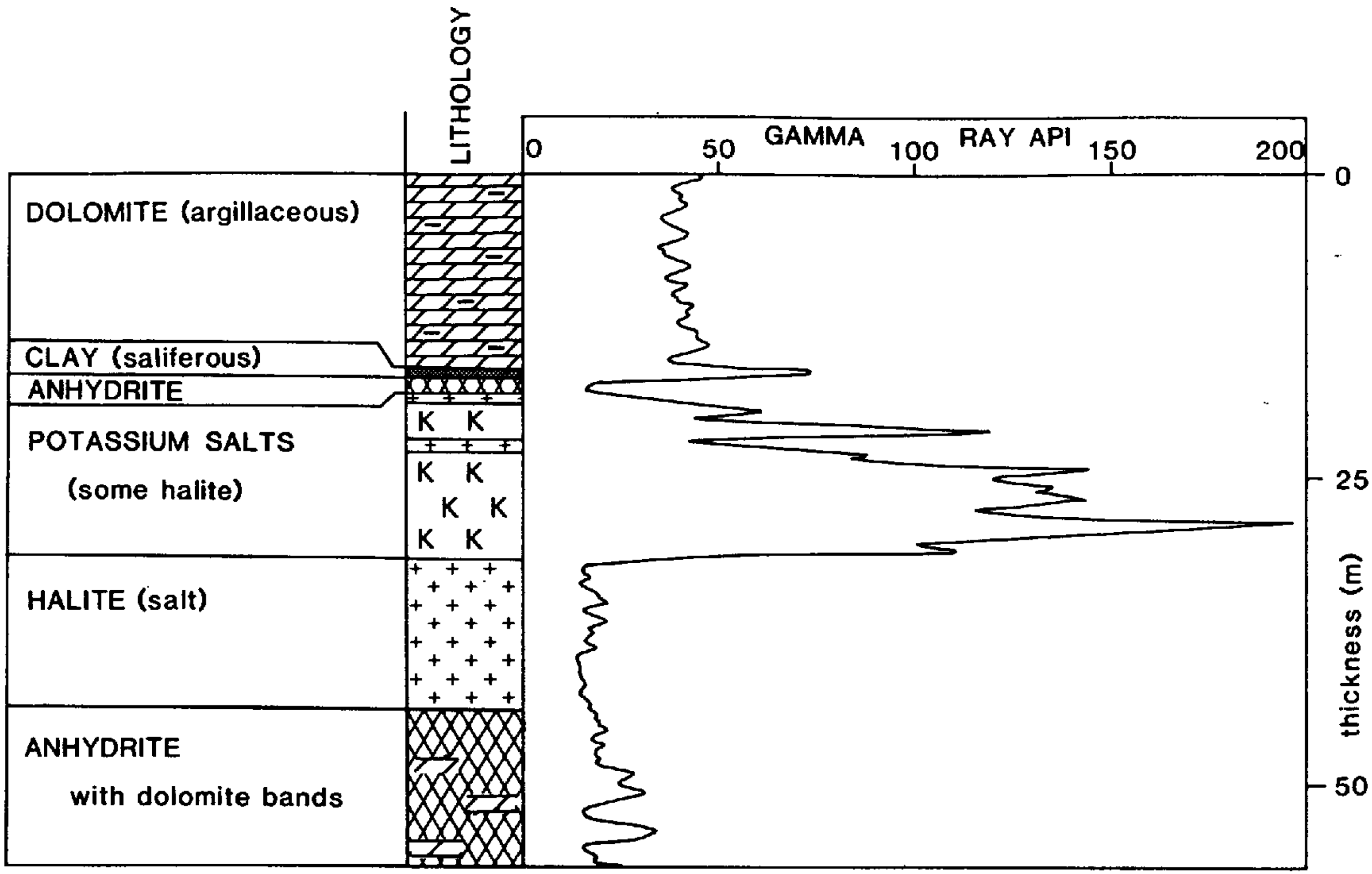

Figure 7.21 Potassium salts giving very high peaks of radioactivity in an evaporite sequence. (The lithology comes from an interpretation of combined logs and cuttings). Permian, North Sea.

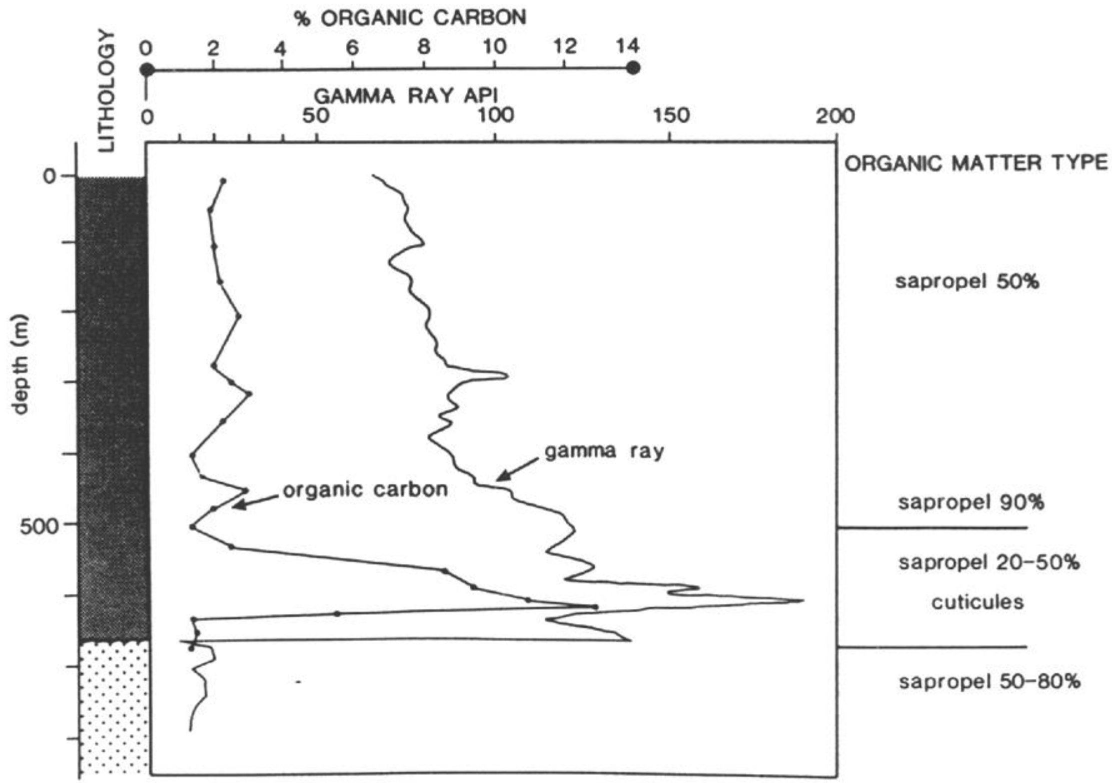

Figure 7.22 High organic carbon values and the total gamma ray giving good correlation, in this case due to uranium associated with organic matter.

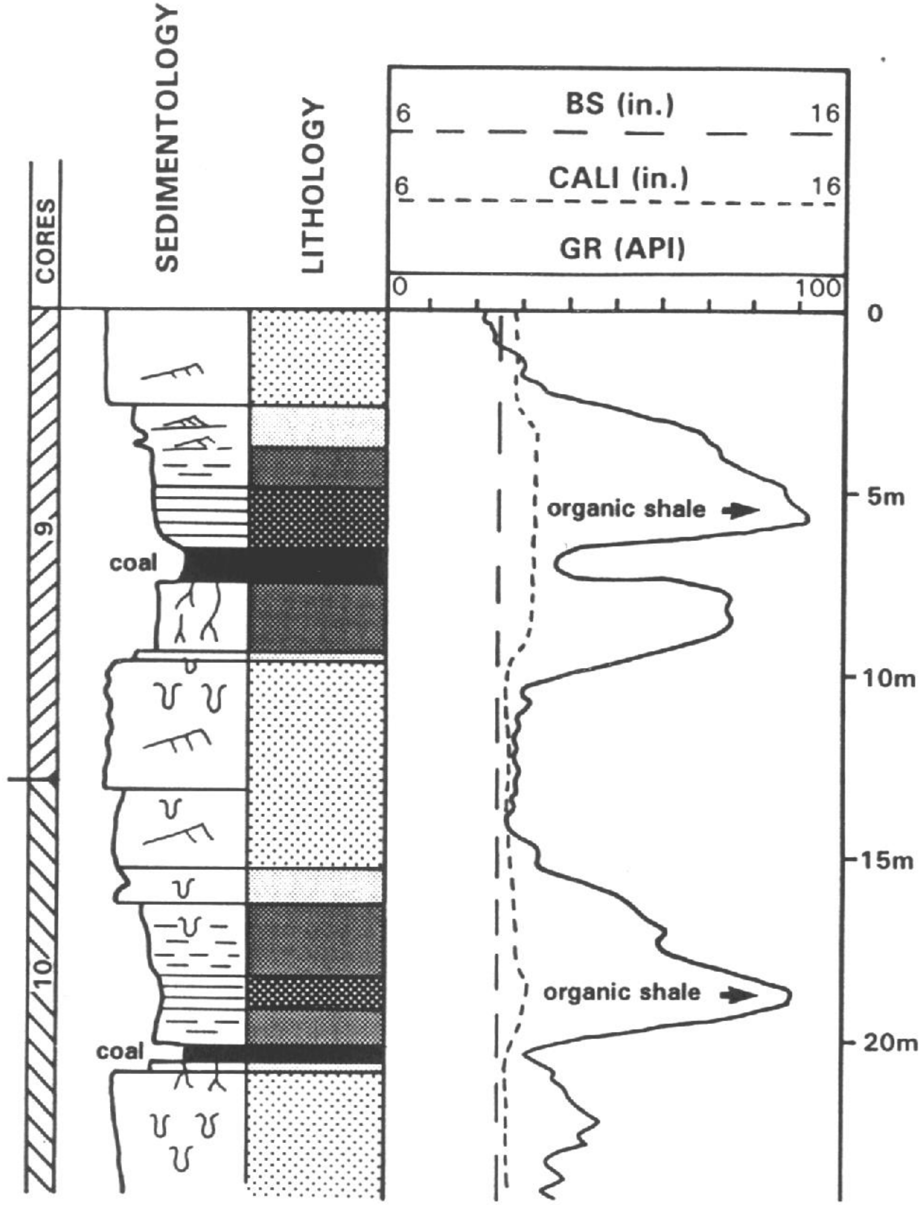

Figure 7.23 Gamma ray characteristics of coal (very low values) and organic rich shale (very high values) in a deltaic sequence.

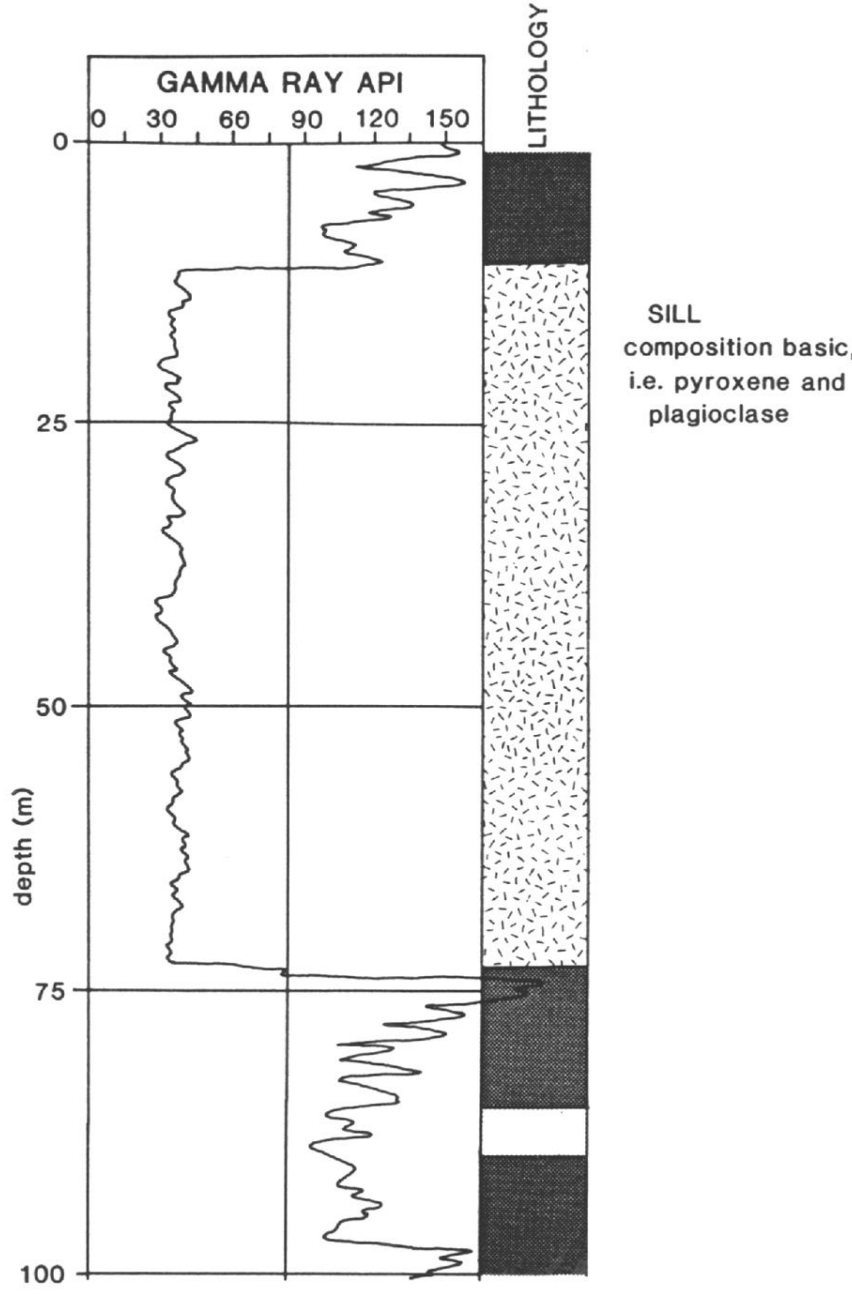

Figure 7.24 Low gamma ray values through a basic sill. It may be confused with a sandstone interval.

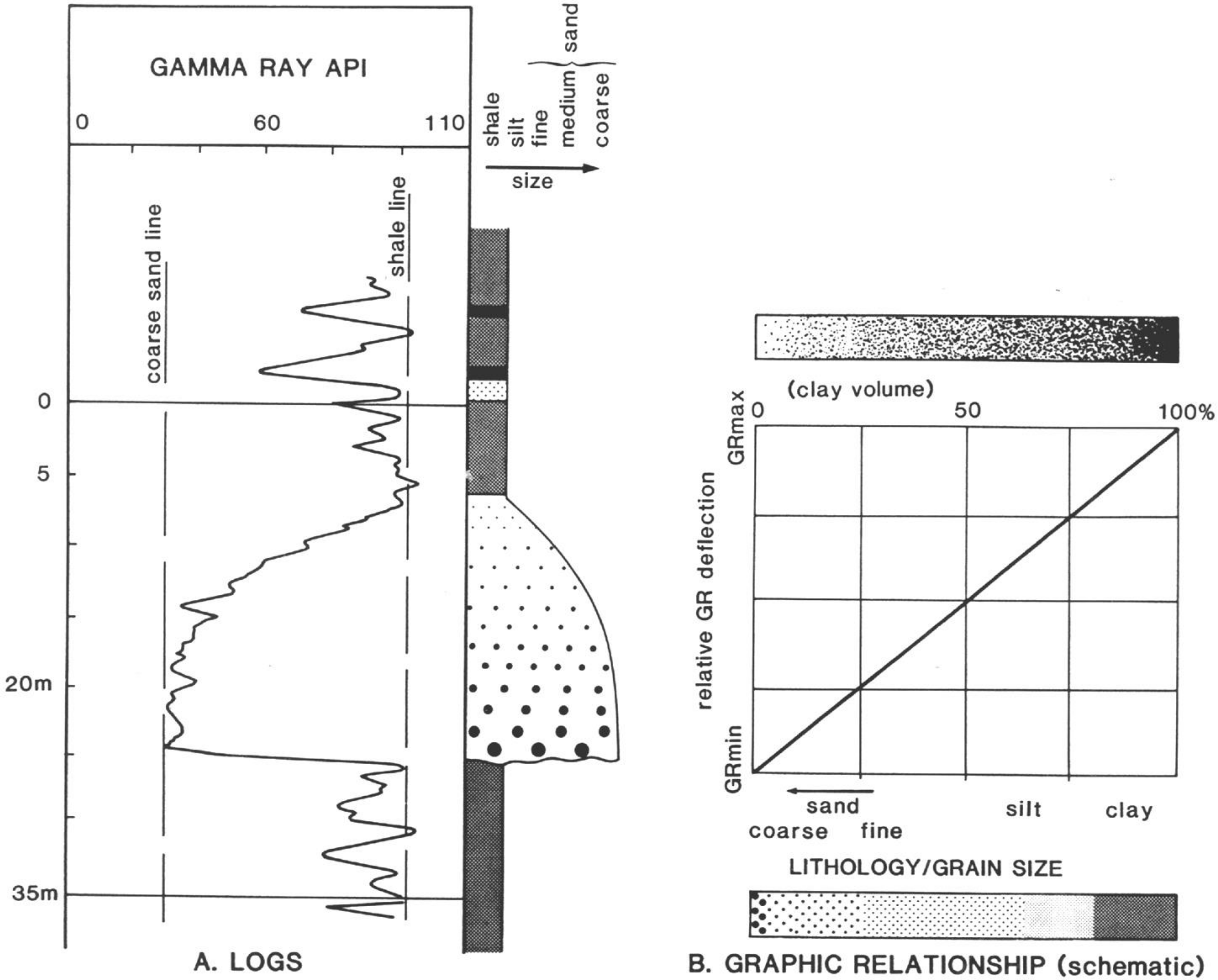

Figure 7.25 Facies from the gamma ray log. (A) The changes in sandstone grain size are reflected in changes in the gamma ray value. This allows a facies to be suggested. (B) Graphic representation of the variation of grain size with gamma ray value. Here it is expressed as a straight line but the relationship is very variable. It should parallel the clay volume change.

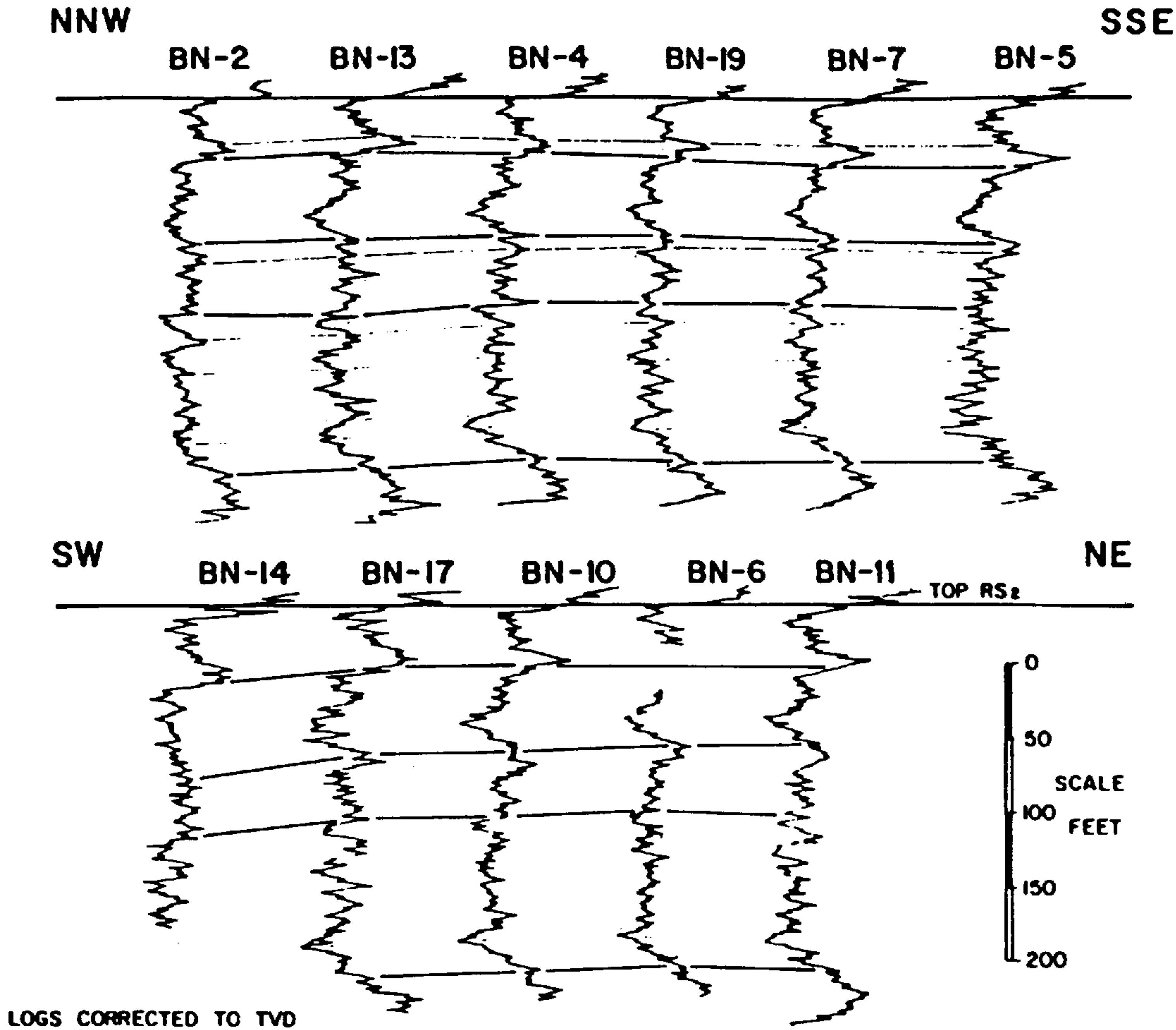

Figure 7.26 Correlation using the gamma ray log. Baronia field, Sarawak. (From Scherer, 1980).

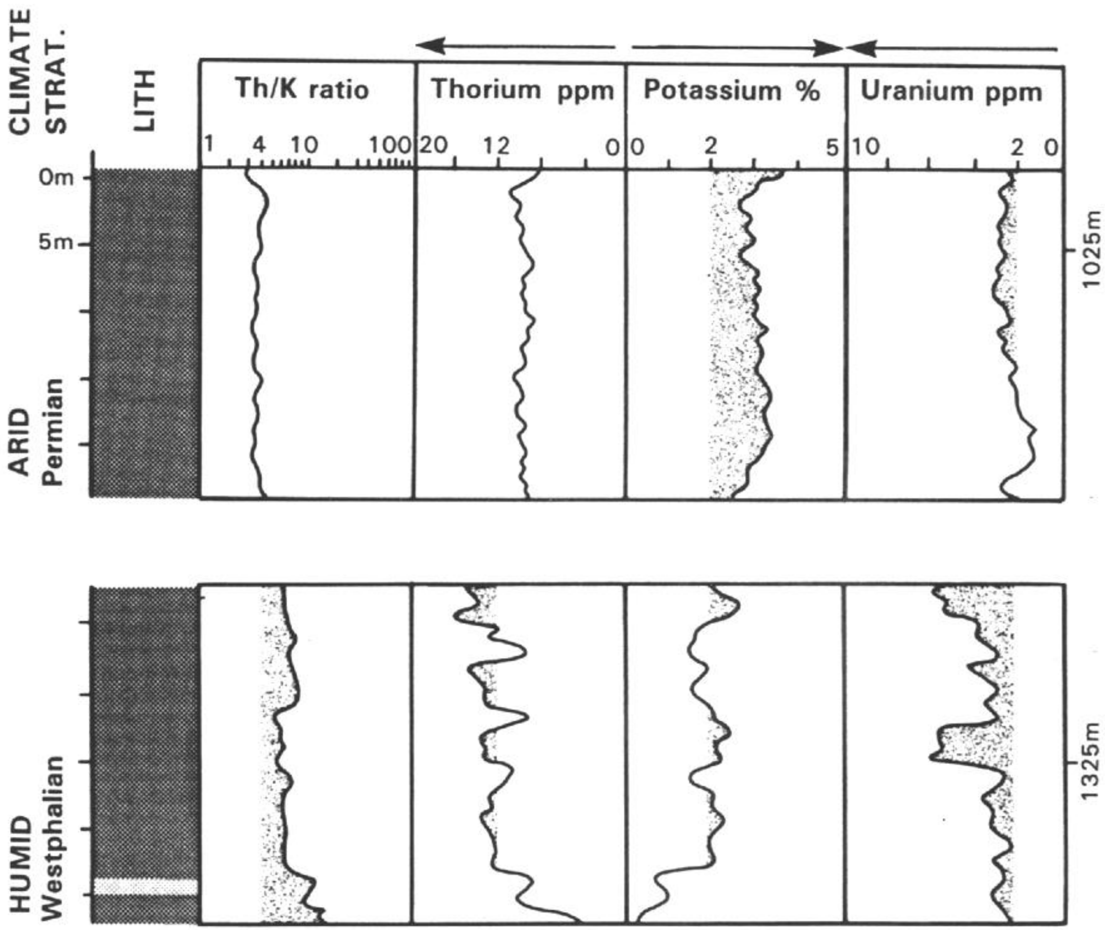

Figure 7.28 Thorium/potassium, Th/K ratio changes in shales, associated with climatic variation. High ratios are associated with a humid climate (abundant kaolinite) low values with an arid climate (abundant illites). Westphalian and basal Permian, central UK.

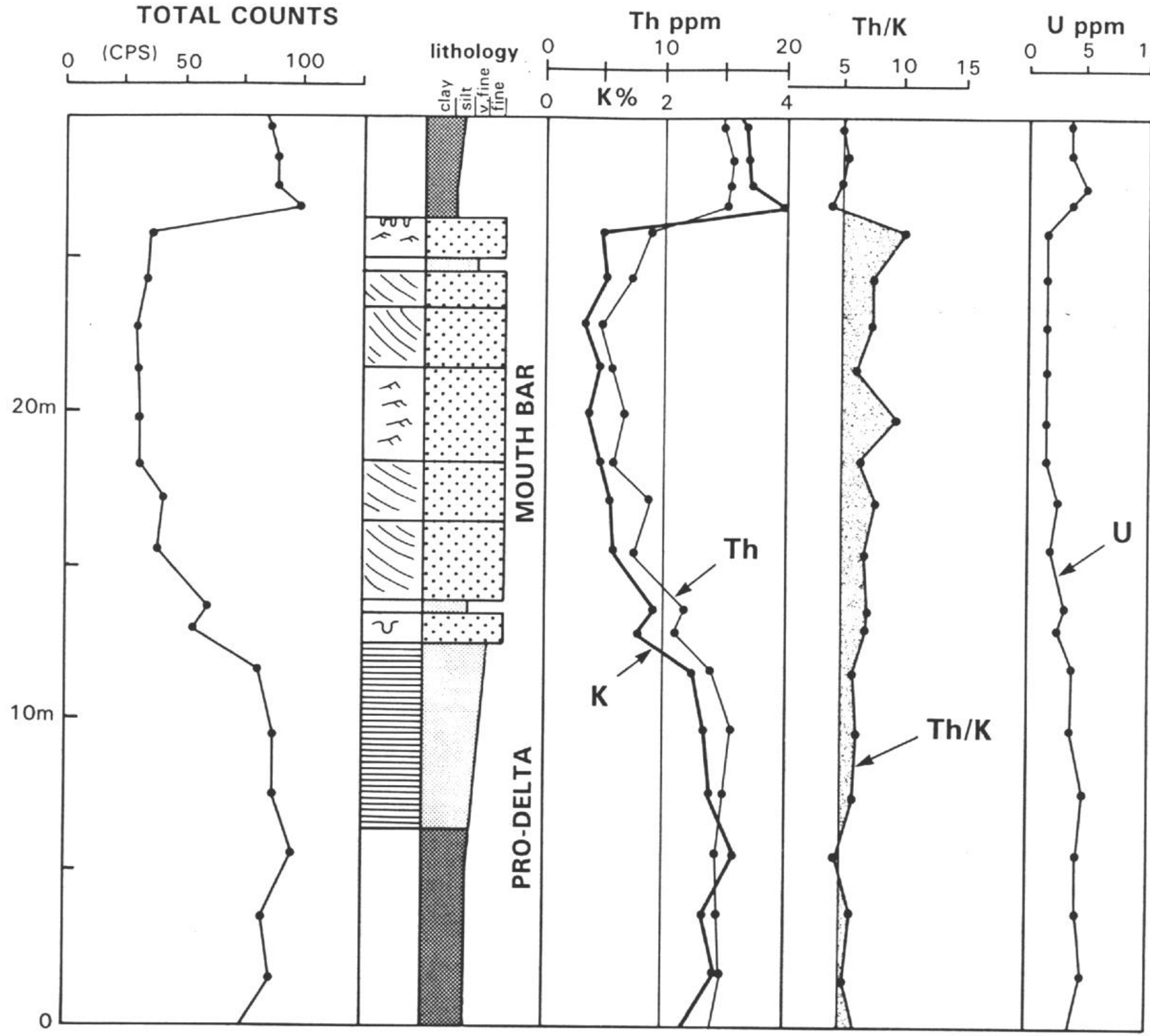

Figure 7.29 Thorium/potassium, Th/K ratios in silts and sands associated with change in grain size. Thorium is relatively more abundant in coarser grained fractions when sediment source is constant (Namurian outcrop, Co. Clare, Ireland, from Myers, 1987).

LITHOLOGICAL SYMBOLS

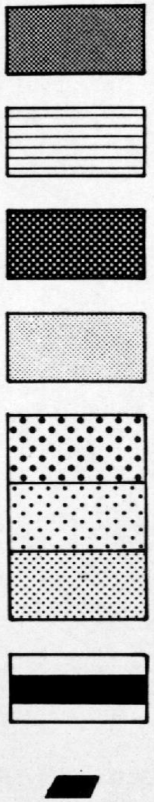

- Shale
- Shale (alt.)
- Organic shale
- Silt
- Sandstone: cse, med., fine
- coal
- coal debris

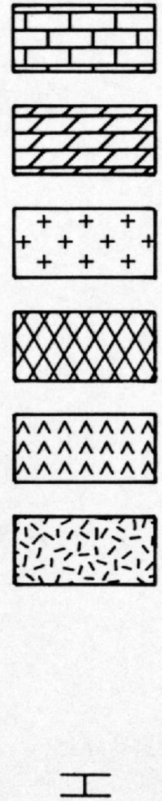

- Limestone
- Dolomite
- Salt (halite)
- Anhydrite
- Gypsum
- Volcanic
- carbonate cement

SEDIMENTARY STRUCTURES

- cross-beds
- ripples: current, wave
- horizontal laminae
- irregular laminae
- concretion
- horizontal burrows

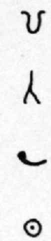

- vertical burrows
- roots
- shells
- oolites

SEDIMENTOLOGICAL FORMAT

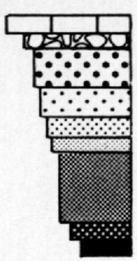

- Carbonate
- cgl
- Sandstones: cse, me, fi
- Silt
- Shale
- Organic shale
- Coal